UiT
THE ARCTIC
UNIVERSITY
OF NORWAY

Faculty of Science and Technology

Department of Mathematics and Statistics

Ice-albedo tipping points in a diffusive energy-balance model with land and ocean

—

Kristian Bergum Hilbertsen

Master thesis in Applied Mathematics MAT-3900, January 2021

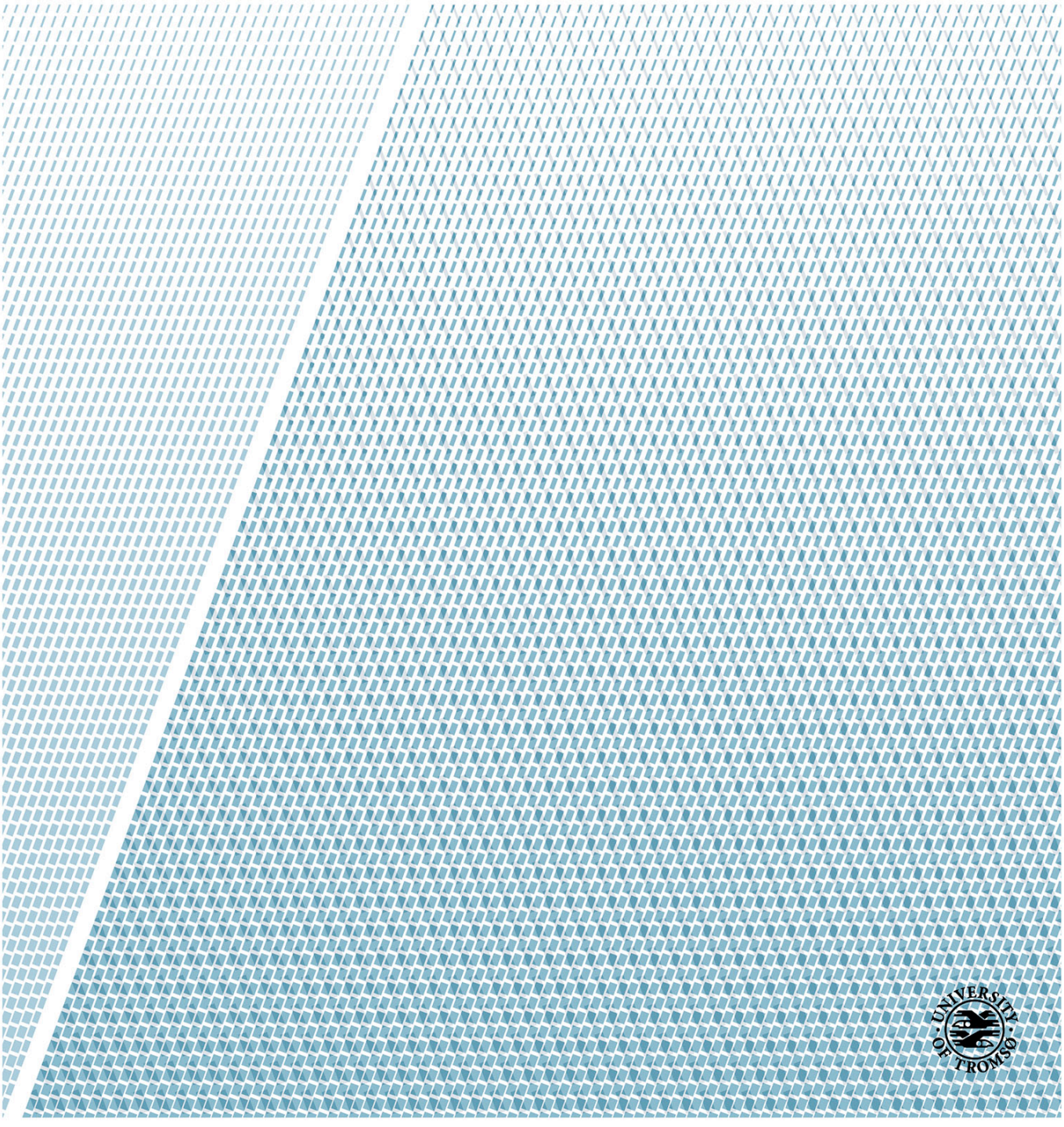

Abstract

The ice-albedo feedback is associated with the nonlinearity in the climate system, due to the sudden change in albedo between ice-free and ice-covered surfaces. This nonlinearity can potentially cause abrupt and dramatic shifts in the climate, referred to as tipping points. It is also believed that this mechanism has contributed significantly to the precipitous losses of Arctic sea ice, which have outpaced the projections of most climate models.

This feedback mechanism has been studied since at least the nineteenth century, and it has had a major role in climate science ever since. The tipping points that result from this mechanism has changed the way we view the history of the Earth with the introduction of, among other things, the snowball Earth hypothesis.

In this thesis we will introduce land area to a diffusive Energy Balance Model, and study these critical transitions. We will also test for Early Warning signals for these tipping points.

Acknowledgements

I would like to thank everyone who has helped me complete this project, whether it be proofreading or listening to me complain about my program not running properly.

A special thanks to my supervisor Martin Rypdal, who has introduced me to many new and interesting areas of mathematics and climate science. His great advice and ideas has been vital to the completion of this thesis.

Contents

List of Figures

List of Tables

Chapter 1

Introduction

In the 1960s and 1970s, mathematical modeling of the climate received renewed interest due to the concern over anthropogenic climate change. The evolution of high-speed computers and the development of numerical weather prediction models meant that we could start to simulate the Earth's complex climate. Today our computers are far better and can handle much more complex models and calculations than computers from the 70s. However, to make progress with the complex climate models, the simpler members of the model hierarchy must be thoroughly analyzed [1].

These simple models, as well as geological findings, showed that Earth's climate had gone through several dramatic shifts, like the great oxidation when the level of oxygen in the atmosphere suddenly and irreversibly went from a state of 10^{-5} times the current level of oxygen to one with 1 to 10% of the current level [2]. They also showed that the Earths climate has transitioned to and from a climate state called snowball Earth. In this thesis, we will use a diffusive energy balance model introduced by Gerald North [3] and explore some of these dramatic shifts of the Earths climate.

This model has been used to study, among other things, the small ice-cap instability. Therefore it assumes a planet entirely covered in water. This thesis will add more realism to the model by introducing land surface and exploring how this influences abrupt transitions caused by the ice-albedo feedback. We will then focus on the transitions to and from snowball Earth and see if we can observe early warning signals for these transitions.

This thesis will focus on three climate science concepts, which will be explained in more detail later in a later chapter, but they will be introduced briefly here.

1.1 The Energy Balance Model

The models referred to as Energy Balance Climate models (EBMs) are at the lower end of the model hierarchy, meaning they are more simplistic than other climate models. They are conceptually simple[1] because they are based on a single equation. The temperature change is only dependent on the energy absorbed by the Earth versus the energy radiated from Earth. If Earth absorbs more than it disperses, the Earth gets warmer and vice versa.

1.2 Tipping points

A tipping point (TP) is a threshold where a small change can push a system into a different state. It can be thought of as a child going down a slide; there is a point at which it is too late for the child to stop from sliding down. At this point, the child travels inevitably towards a different state. It ends up at the bottom.

Early studies of potentially irreversible TPs focused on the transition to the Snowball Earth state[4][5]. This transition is one of the focuses of this thesis. In recent years, researchers have focused on answering whether external causes or internal mechanisms cause climate fluctuations and transitions between different states. External causes may be variations in the Earth's orbit, and internal causes can be changes in the time scale of atmospheric or oceanic feedback.

1.3 Early Warning Signals

TPs can have dramatic consequences, and even though they may be inevitable in some cases, we want to predict when or if this might happen. This is our motivation for searching for EWS. There are several methods that can be used for detecting EWS that will be discussed further. In this thesis we will focus on the following methods:

Slow recovery from perturbations as a system approaches a TP; the potential well gets shallower and wider. This means that the system can oscillate slower in the well, leading to slower recovery time.

[1] Though they may be conceptually simple, the mathematical methods for solving can be very complex

Increase in variance when the well gets wider, the system may move further from the stable state.

Increase in autocorrelation as the system recovers more slowly.

1.4 Outline

Chapter 2 introduces Energy Balance models. This chapter aims to explain how they work and what we can learn from them.

Chapter 3 describes the model used in this thesis.

Chapter 4 introduces the concept of tipping points and discusses tipping points in Earth's climate.

Chapter 5 introduces the model parameters used in this thesis and then shows the results from the different cases explored, using the model from chapter 3.

Chapter 6 discusses methods for observing Early Warning Signals for tipping points and the validity of these methods.

Chapter 7 applies Early Warning Signals to some of the results from chapter 5.

Chapter 8 discusses the results from chapter 4 and 7.

Chapter 9 summarises the findings in this thesis and discusses their implications and some ideas about further work.

Chapter 2

Energy Balance Models

This chapter aims to explain how an Energy Balance Model works. It does so by using a simple example to introduce some of the climate phenomena explored in this thesis.

2.1 Simple Energy Balance Model

EBMs were introduced by Budyko [6], and Sellers [7] independently. They describe the balance of the Earth's energy budget. The simplest of these models depict the change in global temperature as the incoming and outgoing radiation energy flux:

$$c\frac{dT}{dt} = E_{in} - E_{out}\,, \tag{2.1}$$

where c is the heat capacity, which dictates the response time of the temperature T. Equation 2.1 says that the change in temperature is proportional to the difference of absorbed and radiated energy.

The term E_{in} is the energy absorbed by the Earth from the sun. However, not all the incoming energy is absorbed by the Earth and turned into heat. About 30% of the incoming solar radiation is reflected back into space [8]. The proportion of incoming radiation that is reflected is called the albedo, and the proportion absorbed by the Earth is called co-albedo. E_{in} can be defined as the co-albedo times the amount of radiation reaching Earth's surface:

$$E_{in} = (1 - \alpha(T))Q \tag{2.2}$$

Here $1-\alpha(T)$ is the co-albedo, T is the global mean temperature, and $Q = 342\text{Wm}^{-2}$ is a fraction of the solar constant. As a heuristic model we let

$$\alpha(T) = 0.5 - 0.2 \cdot \tanh\left(\frac{T-265}{10}\right) \tag{2.3}$$

This is a smooth function that makes the albedo 0.7 under really cold conditions (Earth covered with ice and snow), and 0.3 under really warm conditions (ice-free Earth).

Like the Sun, the Earth emits electromagnetic radiation. This radiation is dependent on the temperature of the Earth. Using Stefan-Boltzmanns law and assuming that the Earth radiates as a black body, E_{out} can be written as

$$E_{out} = \sigma T^4 \tag{2.4}$$

where σ is Stefan's constant $\sigma = 5.67 \cdot 10^{-8} WM^{-2}K^{-4}$.

Greenhouse gasses affect the the quantity E_{out} but not E_{in}. This needs to be accounted for in even the simplest models. Reducing the expression for E_{out} by a factor ε, can (in a very simplistic way) model the greenhouse effect:

$$E_{out} = \varepsilon\sigma T^4 \tag{2.5}$$

Equation 2.1 becomes

$$c\frac{dT}{dt} = (1-\alpha(T))Q - \varepsilon\sigma T^4 \tag{2.6}$$

This model is a zero-dimensional EBM, which means that the model is only dependent on one scaler variable, namely the temperature T. Even though it is a very simple model, it can be used to illustrate some interesting concepts.

2.1.1 Earth's Equilibria

When the incoming and outgoing radiation are equal we are at an equilibrium state. Using the expressions for E_{in} and E_{out} we have the following equation for energy balance:

$$(1-\alpha(T))Q = \varepsilon\sigma T^4 \tag{2.7}$$

Plotting E_{in} and E_{out} together shows something very interesting.

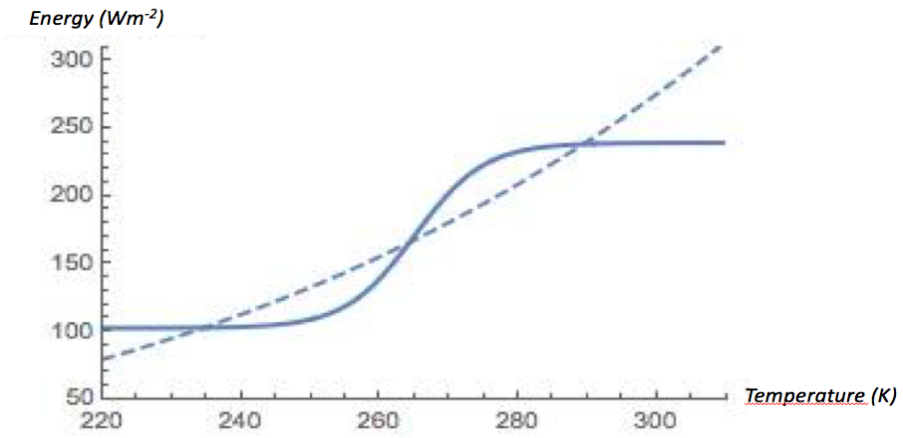

Figure 2.1: E_{in} vs E_{out} shows that the Earths climate system can have multiple equilibria.

Figure 2.1 shows the E_{in} as a thick solid curve, and E_{out} as the dotted line. The three points of intersection corresponds to the three equilibrium states: $T_1^* \approx 235K$, $T_2^* \approx 265K$ and $T_3^* \approx 285K$. The temperature T_3^* corresponds roughly to the current climate, and T_1^* to a snowball-Earth climate. The temperature T_2^*, however, is an unstable solution, which cannot persist and will never be observed.

If the climate system is in the equilibrium state at T_2^*, and the temperature increases slightly, the right hand side of equation 2.6 becomes positive. If the temperature decreases slightly, the right hand side of 2.6 becomes negative. This means that a small perturbation in T will cause a runaway effect that would force the climate system away from the equilibrium state T_2^*. An unstable equilibrium can be thought of as a pencil balancing on its tip. The pencil is perfectly still, but a small gust of wind can cause it to fall over.

2.2 The Snowball-Earth Hypothesis

Snowball Earth is a state where the entire Earth is covered in ice and snow, making it look like a giant snowball. The EBM discussed above suggests this is a stable equilibrium point for Earth's climate. In fact, our planet may have been entirely covered in ice and snow, perhaps multiple times.

An ice-covered Earth would reflect a large proportion of incoming solar radiation back into space. Only a small fraction of the energy would be absorbed; hence the climate will be very insensitive to variations in incoming radiation from the sun. This feedback mechanism makes snowball Earth

very stable, and a large event would be needed to escape from the locked-in state. One such event may have been one or more large volcanic eruptions [9]. Such eruptions would increase the amount of CO_2 in the atmosphere, increasing the greenhouse effect and resulting in the Earth heating up.

The paper by Yves Goddéris et al. [10] summarizes three scenarios that have been suggested and numerically tested to explain how and why the Earth transitioned to a snowball-Earth state. All of these scenarios rely on large drops in the partial pressure in greenhouse gasses.

The snowball Earth bifurcation can be simulated by EBMs (as shown above) and simple General Circulation Models (GCM). However, according to Paulsen et al. [11] a fully coupled GCM is not able to produce ice at the equator. Even though some of the models disagree as to whether the Earth has ever been in a snowball-Earth state, there is some geological evidence that the Earth was in this state in the Neoproterozoic era, more than 500 million years ago [12]. This evidence is one of the many reasons why an EBM was used in this thesis instead of the far more complex GCMs and Earth System Models (ESMs). These complex models are fairly reliable for our current climate, but they fall short when simulating an entirely different climate state.

2.3 Other Models

EBMs are not the only models used to study the climate, but they are the simplest. EBMs are entirely built on the principle in equation 2.1. This simplicity put some restrictions on EBMs. For instance, it is impossible to use an EBM to predict changes in atmospheric and oceanic circulation. For cases like this, it is better to use an ESM that seeks to simulate all relevant aspects of the Earth's climate. They use physical, chemical, and biological processes to achieve this level of detail. The sophistication level allows them to represent human influence on the climate better than both EBMs and GCMs. GCMs are between EBMs and ESMs in the model hierarchy and use physical processes in the atmosphere and ocean to model Earth's climate. Therefore ESMs have the atmospheric and oceanic components of a GCM, but they include other factors of the Earths climate as well.

Even though EBMs are excellent tools for modeling the climate, they have limitations. For one, EBMs work best for the surface-temperature field. Trying to include the rest of the atmosphere into the model introduces a host of new mechanics and complexity to the model.

One might think to add all the known mechanics and factors of the climate system to a single ”perfect” model. However, apart from such a models computational cost, there is another problem: As new physical processes are introduced to a model, even more parameters have to be introduced and calibrated. This process may lead to a problem known by statisticians as overfitting or overtuning. Overfitting will arise when parameter selection does not correctly account for the observations and model structural uncertainties. Then, tuning may become an error compensation rather than a model calibration.

Simple EBMs are always highly idealized, but can give us some insight into the dominant features of our very complex climate system.

Using EBMs has two major benefits:

- Relatively short run-time
- Changes in results can easily be traced back to the change made

Both of these benefits result from the models simplicity and allow studying particular processes in the climate. These results can be used to help the development of more complex models that are more costly to run.

Chapter 3

The Diffusive Energy Balance Model

This chapter will introduce the model used to produce the results for this thesis. It will also explain how the model had to be changed to include land area in a model that initially assumed an Earth entirely covered by water.

3.1 Norths Model

The EBM summarised in the article by North [3] is described by a single partial differential equation:

$$c\frac{\partial T}{\partial t} = -A - BT + \alpha S + D\nabla^2 T + F \tag{3.1}$$

where $-A - BT$ is the top-of-atmosphere outgoing longwave radiation, αS is the incoming radiation multiplied with the co-albedo (the absorbed radiation from the sun), $D\nabla^2 T$ is the transport of heat, and F is additional forcing.

Like the model shown in Chapter 2, this model has incoming and outgoing radiation. However, the transport of heat adds another level of realism and complexity to the model.

3.1.1 Outgoing Longwave Radiation

A linear representation of the top-of-the-atmosphere outgoing longwave radiation was suggested by Budyko [6]:

$$-A - BT$$

The two parameters, A and B, can be fitted to observed data. A typical value for B is $1.9^{-2}C^{-1}$[13], and a typical value for A $211Wm^{-2}$[13].

3.1.2 Solar Radiation

Incoming solar radiation S is constant in longitude but not in latitude. Consequently, S only depends on x. Following the article by North [14] we use

$$S(x) = 1 + S_2 P_2(x)$$

where S_2 is a parameter and $P_2(x)$ is the second Legendre polynomial describing how the incoming solar radiation per unit area is higher at the equator and gets lower towards the poles. This effect is due to the angle of the area relative to the sun. When viewed from the Sun, an area close to the poles will appear smaller than the same area at the Equator. This is due to the curvature of the Earth, which also means that less radiation will hit an area closer to the poles.

Another consequence of the Earths curvature is that radiation will go through more of the atmosphere before hitting an area close to the poles. More of the radiation will be either reflected or absorbed by the atmosphere, reducing the amount of absorbed radiation at the surface.

3.1.3 Co-Albedo

In reality, a lot of the incoming radiation is absorbed by clouds and water vapor. However, in this thesis's idealized models, we ignore clouds and let all radiation reach the surface. The co-albedo is therefore only dependent on if the incoming radiation reaches ice, land, or sea.

In this model, ice is simply implemented as a change in co-albedo in areas cold enough to form ice. This differs from certain other models, such as the model used by Wagner and Eisenman [15], which is a somewhat complex model. In their paper [15] they calculate both ice area and ice volume.

3.1.4 Heat Transport

The diffusive term in the article by North[14] assumed only northward transport of heat. This assumption is valid if there is spherical symmetry, for example a water-covered planet. With the introduction of land, the planet is no longer symmetrical, and heat transport in all directions must

be considered. For a sphere, the heat transport is

$$D\nabla^2 T = D\left[\frac{1}{r}\frac{\partial^2}{\partial r^2}(rT) + \frac{1}{r^2\sin\theta}\frac{\partial}{\partial\theta}\left(\sin\theta\frac{\partial T}{\partial\theta}\right) + \frac{1}{r^2\sin^2\theta}\frac{\partial^2 T}{\partial\varphi^2}\right] \tag{3.2}$$

where T is the surface temperature and D is a thermal diffusion coefficient. The temperature T is measured at sea level, which is at a constant radius. Therefore the temperature will not be dependent on the radius.

By defining $x = \cos\theta$ with latitude θ, and $y = \varphi$ with longitude φ, and using finite differences, the heat transport becomes

$$\begin{aligned} D\Bigg[&\left(\frac{x_i}{\Delta x} + \frac{1-x_i^2}{\Delta x^2}\right)T_{i-1,j} - 2\left(\frac{1-x_i^2}{\Delta x^2}\right)T_{i,j} \\ &+ \left(-\frac{x_i}{\Delta x} + \frac{1-x_i^2}{\Delta x^2}\right)T_{i+1,j} + \left(\frac{1}{1-x_i^2}\right)\frac{T_{i,j+1} - 2T_{i,j} + T_{i,j-1}}{\Delta y^2}\Bigg] \end{aligned} \tag{3.3}$$

Here i is the latitudinal position, j is the longitudinal position, $\Delta x = 1/n$ and $\Delta y = 2\pi/m$. We let n denote the number of grid cells in latitudinal direction and m is the number of grid cells in longitudinal direction.
In this thesis the thermal diffusion coefficient is dependent on space, this is due to the difference of the thermal diffucivity of land and ocean.

In reality, heat transport happens through many different phenomena, but primarily due to Hadley circulation and ocean currents.
If the sea-ice and glaciers melt due to global warming, these ocean currents could weaken and they may disappear. Caesar et al. [16] found evidence for a weakening of the Atlantic Meridional Overturning Circulation by about 3 ± 1 sverdrups (about 15%). This weakening was a feature predicted by climate models in response to rising CO_2 levels. Even though it cannot be ruled out entirely, they concluded natural variations was not the cause of this weakening, but rather a rise in CO_2 levels.

3.2 Modeling the Earth

For this model to work, we need a map of the Earth. Mathematica has a function that gives the elevation of a point above sea level. This function was used to classify each grid cell as land or ocean.

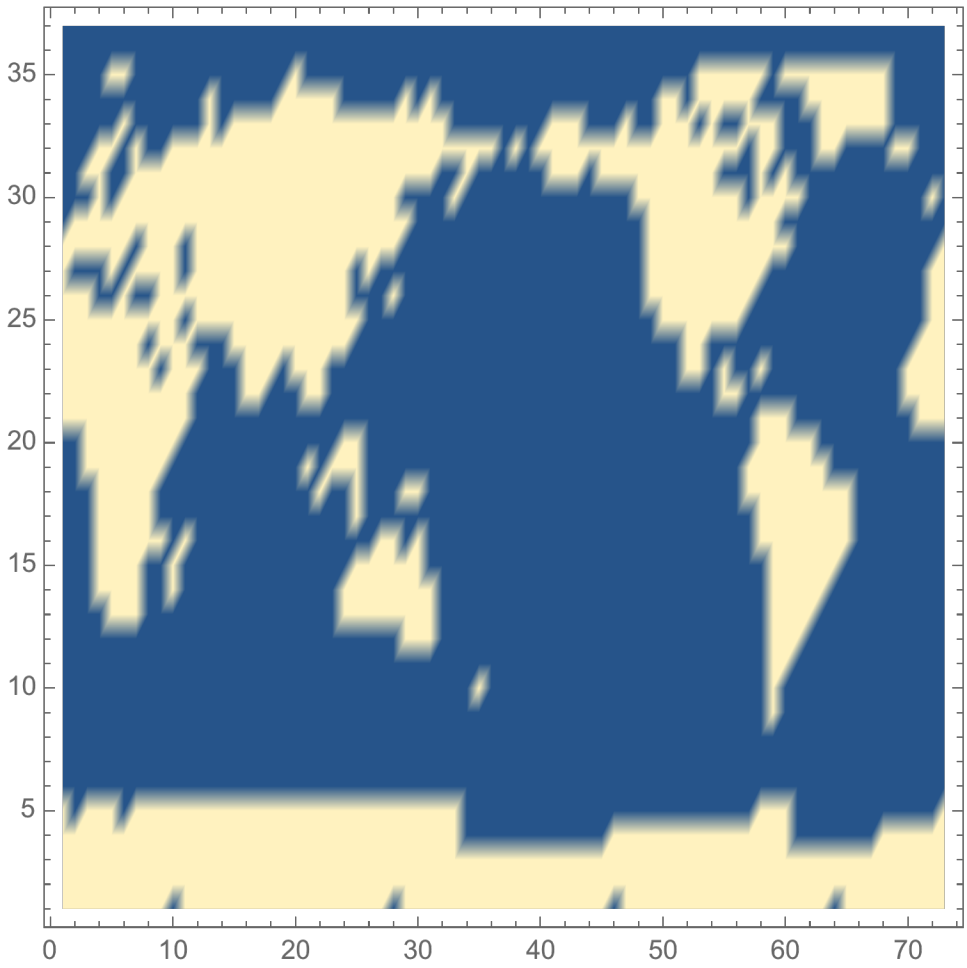

Figure 3.1: Map of the Earth used in this thesis, blue means ocean and yellow means land

3.2.1 Area of the grid cells

The map of the Earth used in this thesis is like many other maps, a plane. However, as cartographers know, it is impossible to map a sphere onto a plane while keeping the proportions correct. Areas close to the poles appear bigger on the map than they are. To get the area of the grid cells to be the correct size we used

$$A = \frac{\pi}{180} R^2 |\sin\theta_1 - \sin\theta_2| \cdot |\varphi_1 - \varphi_2|$$

Chapter 4

Tipping Points

In this chapter, we will explain some of the mathematical theory of tipping points.

4.1 Bifurcation Theory

A bifurcation in climate dynamics is often referred to as a tipping point. A TP is when a physical parameter crosses a threshold that changes the system to a new state that differs considerably from the previous.
The nonlinear differential equations

$$\dot{\mathbf{T}} = f(\mathbf{T}, \lambda) \tag{4.1}$$

where $\mathbf{T} : \mathbf{t} \mapsto \mathbf{T}(\mathbf{t}) \in \mathbb{R}^n$ and $\lambda \in \mathbb{R}^n$ has equilibrium solutions $\mathbf{T}^*$. These solutions can be found (as was done in Chapter 2) by solving the equation

$$f(\mathbf{T}, \lambda) = 0 \tag{4.2}$$

Consider the following scalar ordinary differential equation with a cubic nonlinearity

$$\dot{x} = \mu + x - x^3 \tag{4.3}$$

Here, the equation $f(\mu, x) = 0$ has two solutions for $\mu = \pm\mu^*$, these results are summarised in Figure 4.1.

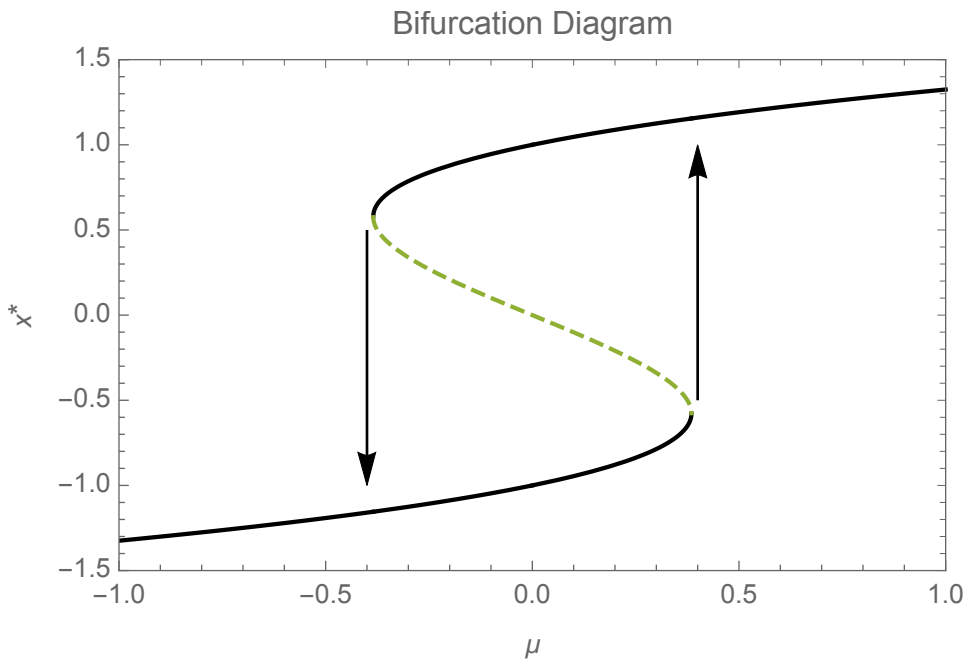

Figure 4.1: Bifurcation diagram with hysteresis loop, black solid lines are stable solution and dashed green is unstable

A bifurcation diagram shows the plot of fixed points x^* against the bifurcation parameter μ. If the system starts with a large value of μ, the system will be some place on the top solid curve. If μ starts to decrease, the system will "slide" along the solid curve. Once μ passes the value $-\mu^*$, the system will not slide along the dotted line. It will "fall" (transition very quickly) as depicted by the left arrow, to the other equilibrium state, and start "sliding" along the bottom solid line.
At this point, a small change in is not enough to make the system "jump" back up. μ must exceed the value μ^* where it follows the other arrow to the other equilibrium solution. These "falls" and "jumps" are called tipping points, and the curves form a hysteresis loop.

Often in climate dynamics, the bifurcation parameter μ will be a forcing. Forcings are external factors that drive the system. Such factors may be volcanic eruptions, changes in the Earths orbit around the sun, or human-induced factors like changes in atmospheric composition and land use. The number of different forcings is one of the many reasons why the Earths climate is such a complex system.

Bifurcations can only take place in nonlinear systems. The amount of absorbed incoming radiation of the Earth is in the Norths model (and the model shown in chapter 2) dependent on the

co-albedo. The co-albedo depends on the temperature. This dependence gives rise to a nonlinear term in equation 3.1.

4.2 Tipping Points in Open systems

Peter Ashwin et al. [17]. suggest three categories of tipping effects

- ”B-tipping”, in which the output from an open system changes abruptly or qualitatively owing to a bifurcation of a quasi-static attractor
- ”N-tipping”, in which noisy fluctuations result in the system departing from a neighborhood of quasi-static attractor
- ”R-tipping”, in which the system fails to track a continuously quasi-static attractor

According to this classification, the classical fold bifurcation (saddle-node bifurcation) falls in the B-tipping category. In realistic models, tipping effect may be due to a combination of the three mechanisms.

4.3 The Earths Tipping Points

Many parts of the Earth's climate can potentially undergo abrupt transitions due to climate change. Scientists are especially concerned over the potential tipping of the Arctic sea-ice cover and the Greenland ice sheet, due to the impact these changes will have on the climate system [18].
If one component of the Earths system undergoes an abrupt transition, it can cause other critical thresholds to be crossed. For example, if the Arctic sea-ice cover is lost, the amplified warming of the Earth can cause a drought in the Amazon rainforest. This drought can cause the Amazon region to transition to an alternative ecological state, where a savanna replaces the rainforest. The rainforest loss would increase atmospheric CO_2 levels and further accelerate warming of the Earth. A scenario of this type is called an Earth system tipping cascade.

Given the TPs found by Budyko [6] and the transition to and from the ice age, we suspect the tipping points of the global average temperature to have the following shape:

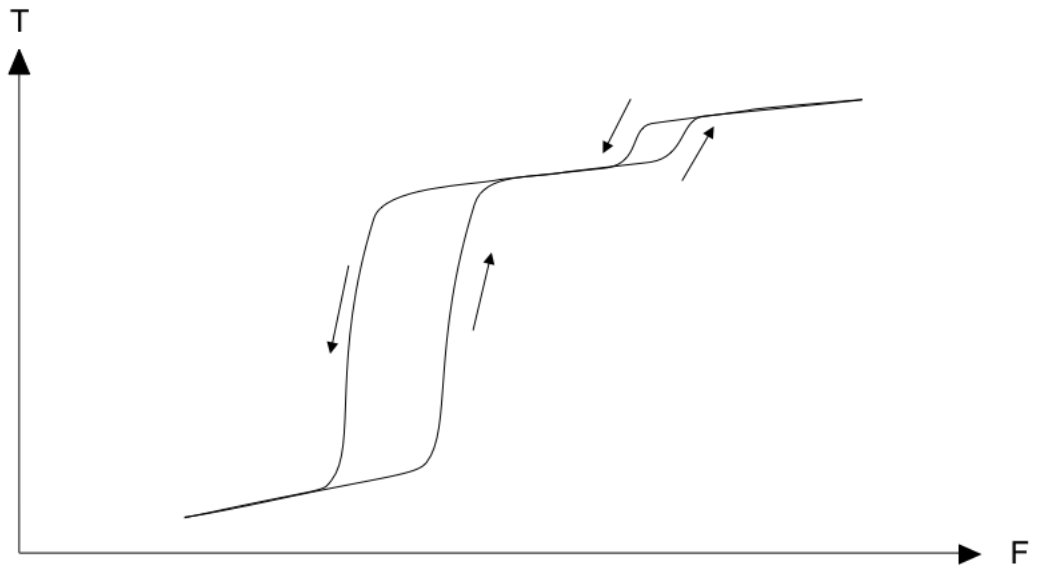

Figure 4.2: Expected temperature profile from forcing

This is very similar to the bifurcation diagram shown in Figure 4.1, but it has two hysteresis loops. We think that this is a transition to and from an ice-age state. This temperature profile will result in melting and forming of ice, which we suspect also will form two hysteresis loops. This bifurcation diagram does not show the unstable solution like Figure 4.1 as it will not be observed.

Chapter 5

Results

In this thesis we analyze the non-linear diffusive energy balance model, and by linearly varying the forcing we study three cases:

- Case 1: Starting from a climate just a little colder than our current climate, we transition to a climate much warmer than ours. Then, we reverse the forcing and cool the Earth back to the starting point
- Case 2: The same as case 2, but we cool the Earth past the starting point and transition to a snowball-Earth state. We then reverse the forcing and warm the Earth back to the starting point
- Case 3: The same as case 2, but assuming that Earth is an aquaplanet (no land and is entirely covered by water/ice).

In the next sections we will first discuss parameter values, and then present the results from these cases, as well as the spatial sensitivity of this model when close to a TP.

5.1 Model Parameters

Before running the model we will justify the values of some of the parameters. Table 5.1 shows the values of the parameters for all the results in this thesis. In the literature, the diffucivity D varies between 0.4 and 0.6[19, 20]. Therefore D was chosen to be within these values.

From North [1] we obtain a value for the coefficient S_2, and in North [3] we find values of land co-albedo α_l, ice co-albedo α_i, and the the incoming solar radiation Q. Sea co-albedo was chosen

Symbol	Description	Value
D_l	Diffucivity on land or ice ($Wm^{-2}K^{-1}$)	0.5125
D_s	Diffucivity in the ocean ($Wm^{-2}K^{-1}$)	0.5
A	Out going longwave radiation at $T = 0$ (Wm^{-2})	200
B	Temperature depedent outgoing longwave radiation (Wm^{-2})	1/0.22
c	Heat capacity	1
S_2		-0.482
α_l	Land co-albedo	0.7
α_i	Ice co-albedo	0.38
α_s	Sea co-albedo	0.8
Q	Amount of solar energy floating into the Earths surface (Wm^2)	334.4
T_{cl}	Temperature at which ice is formed on land (C°)	-3
T_{co}	Temperature at which ice is formed on the ocean (C°)	-5
F	Radiative forcing (Wm^{-2})	Varies

Table 5.1: Parameter values used in the model experiments

to be a little bit higher than land co-albedo, and fitted to obtain the best result. The heat capacity c only changes the response time of the temperature and was normalized to unity. This implies that time is measured in units inversely proportional to the average heat capacity of the climate system.

I also note that the temperature values (in °C) are unrealistic for most of the model experiments in this thesis. The reason for this is that the model is simple and disregards several important feedback mechanisms. Consequently, in the figures, I have chosen to label the temperature and forcing axes with ”arbitrary units” (a.u.). When I refer to a model state being close to the current climate, I mean that the extent of the Arctic sea ice is comparable with current satellite observations.

5.2 Forcing the system

The first model experiments explored the response of a climate close to our own, and the possible ”paths” that the global average temperature can take in response to a increase or decrease in forcing.

The experiment starts with a cold climate that is close to tipping to snowball Earth, but still sta-

ble, and then slowly increasing the forcing linearly to warm it towards current conditions. As this happens, there is an abrupt transition from an ice-age-like state to the current small-ice-cap state.

After the warming is complete, we can linearly decrease the forcing and bring the temperature down.

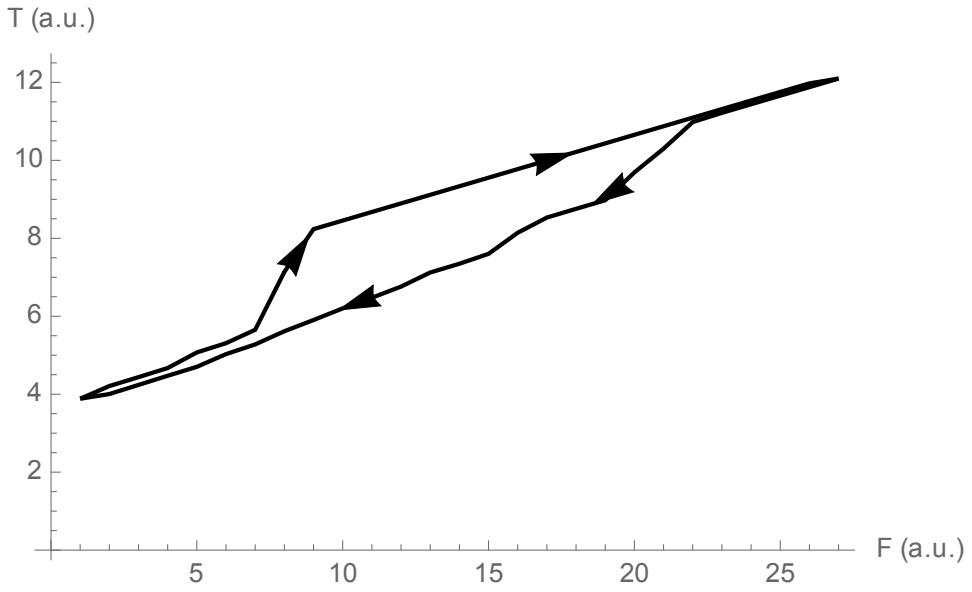

Figure 5.1: Global average temperature response to forcing without transitioning to snowball Earth

As the climate cools it takes a new trajectory in phase space and enters a ice-age-like state through an hysteresis (Figure 5.1).

In Figure 5.2 we observe the same as in Figure 5.1, as well as transitions to and from snowball Earth state.

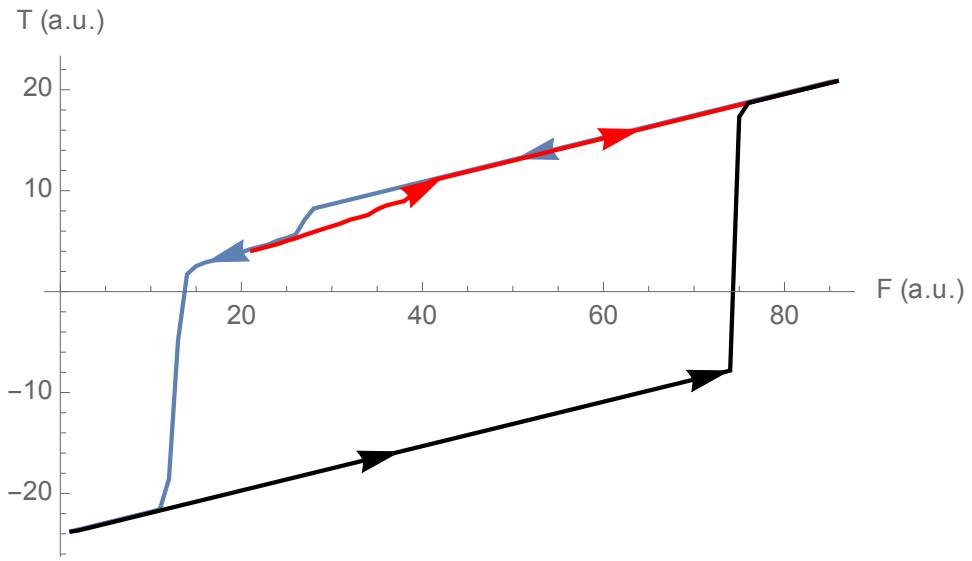

Figure 5.2: Global average temperature response to forcing within our current climate state, and forcing to and from Snowball Earth, with land. Red: From close to TP to warm. Blue: From warm climate to Snowball Earth. Black:From Snowball Earth to warm climate. With land

5.2.1 Ice Area

We can calculate whether or not there is ice in a grid cell by checking if the temperature in the grid cell is lower or higher than the temperature at which ice is formed. Summing the areas of all the grid cells that had ice formation we obtain the extent of ice on the planet. This was done for each time step to get the plot of how the ice area on the Earth responds to a linear forcing.

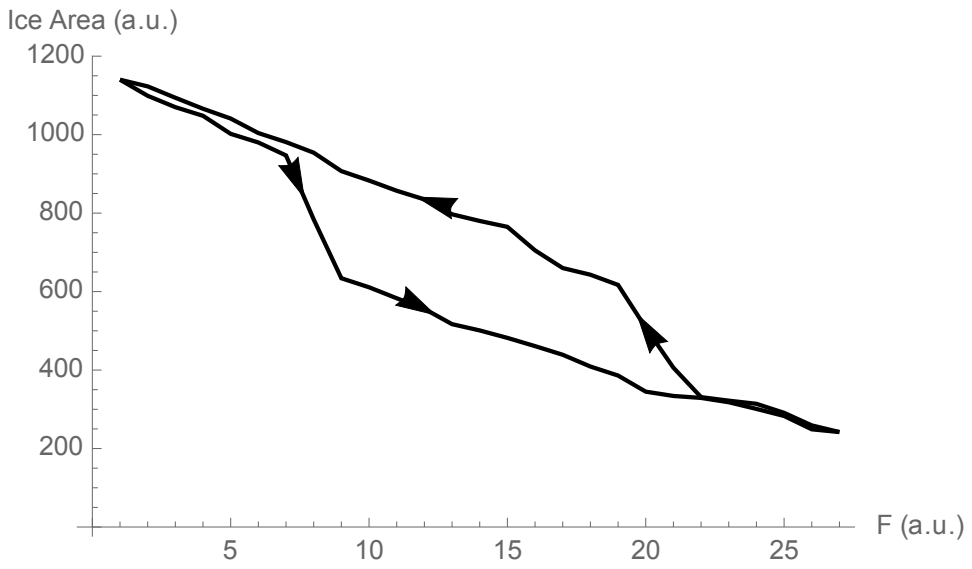

Figure 5.3: Ice area response to forcing without transitioning to snowball Earth

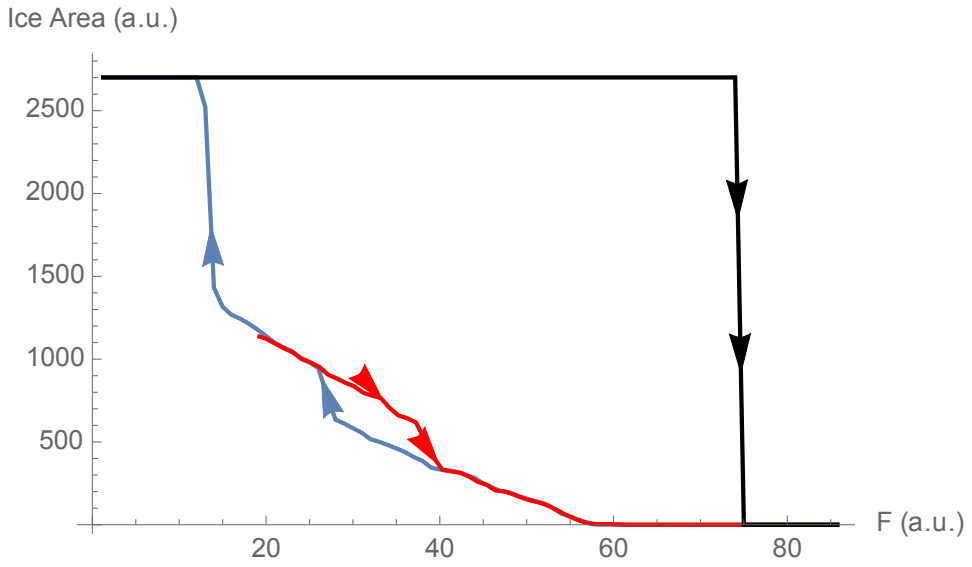

Figure 5.4: Ice area response to forcing within our current climate state, and forcing to and from Snowball Earth. Red: From close to TP to warm. Blue: From warm climate to Snowball Earth. Black: From Snowball Earth to warm climate.

The y-axis shows the number of grid cells with ice, with ”zero” meaning there is no ice on the planet surface and 2701 meaning that every grid cell is covered with ice.

5.3 Forcing the system without land

After removing land in the model (planet entirely covered in water/sea ice) we have spherical symmetry. This means that heat transport does not happen along the latitudes. The results of running the same model without land is summarized in Figure 5.5 and 5.6

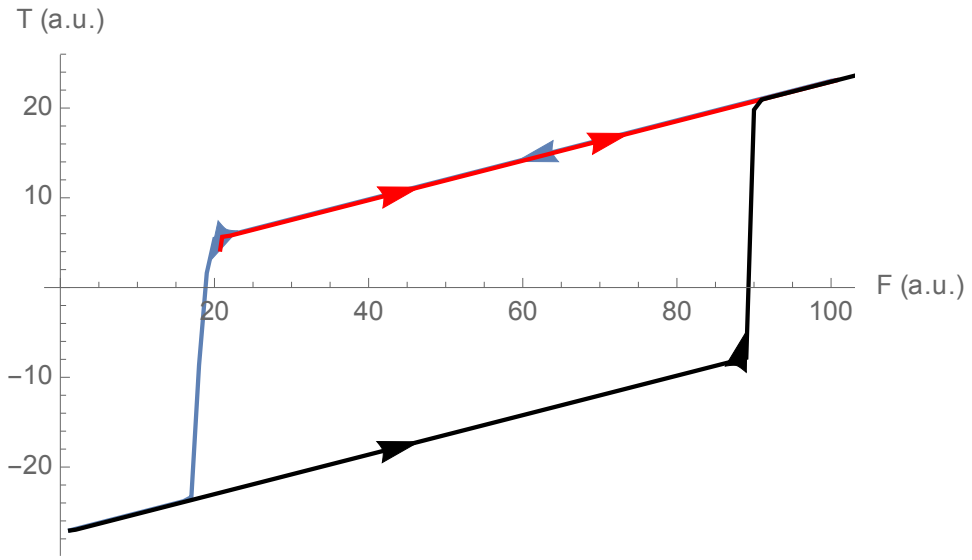

Figure 5.5: Global average temperature response to forcing within our current climate state, and forcing to and from Snowball Earth when the Earth is an aquaplanet. Red:From close to TP to warm. Blue: From warm climate to Snowball Earth. Black: From Snowball Earth to warm climate.

5.3.1 Ice Area

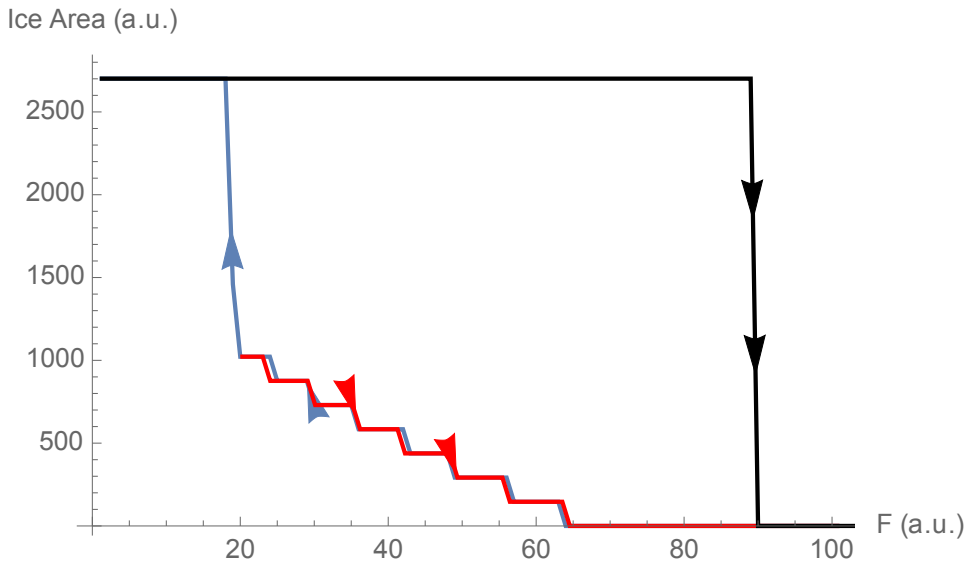

Figure 5.6: Ice area response to forcing within our current climate state, and forcing to and from Snowball Earth when the Earth is an aquaplanet. Red: From close to TP to warm. Blue: From warm climate to Snowball Earth. Black: From Snowball Earth to warm climate.

5.4 Spatial Sensitivity

When Earth's climate is close to a tipping point to (or from) Snowball Earth, some areas are more sensitive to temperature change than other. This means that some areas need a larger temperature change to cause the climate to undergo a state transition. We can perturb the temperature of (relatively) small areas of the planet surface and observe if the entire climate tips. By gradually increasing the size of the perturbation, we can see how sensitive the areas are.

Since the area of the grid cells at the equator are larger than the grid cells near the poles, we need to factor in the area of the grid cells. Therefore the perturbations are on the form

$$F_p = T_p \frac{A_i}{\max A} \tag{5.1}$$

where A_i is the area of the grid cell and $\max A$ is the area of the biggest grid cell. In this thesis, the planet surface was partitioned into 2701 grid cells, meaning the average area for each grid cell is 189 000 km^2.

To obtain a state close to the TP to (or from) Snowball Earth we force the system towards the bifurcation point and stop right before it tips over (also checking that the system is still at a stable solution). Then we perturb the grid cells to see if the climate tips over.

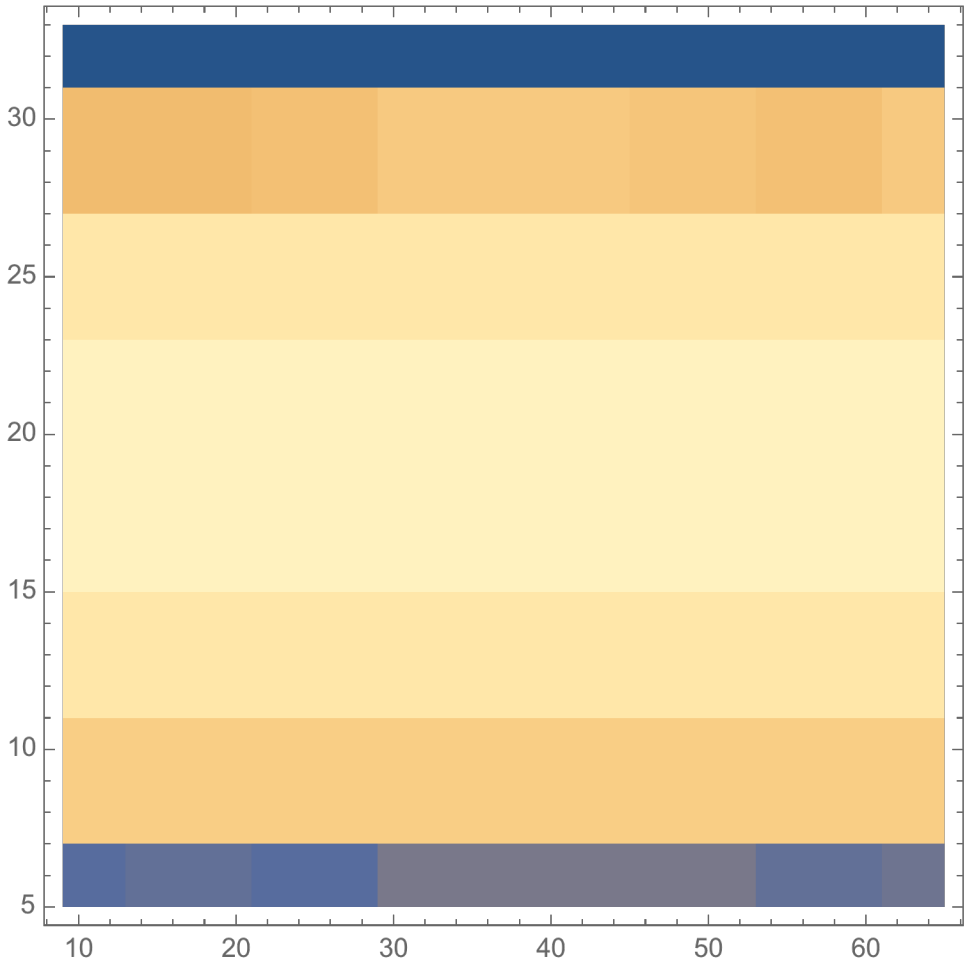

Figure 5.7: Spatial sensitivity when close to tipping from Snowball Earth. Blue is the least sensitive, and white is the most sensitive

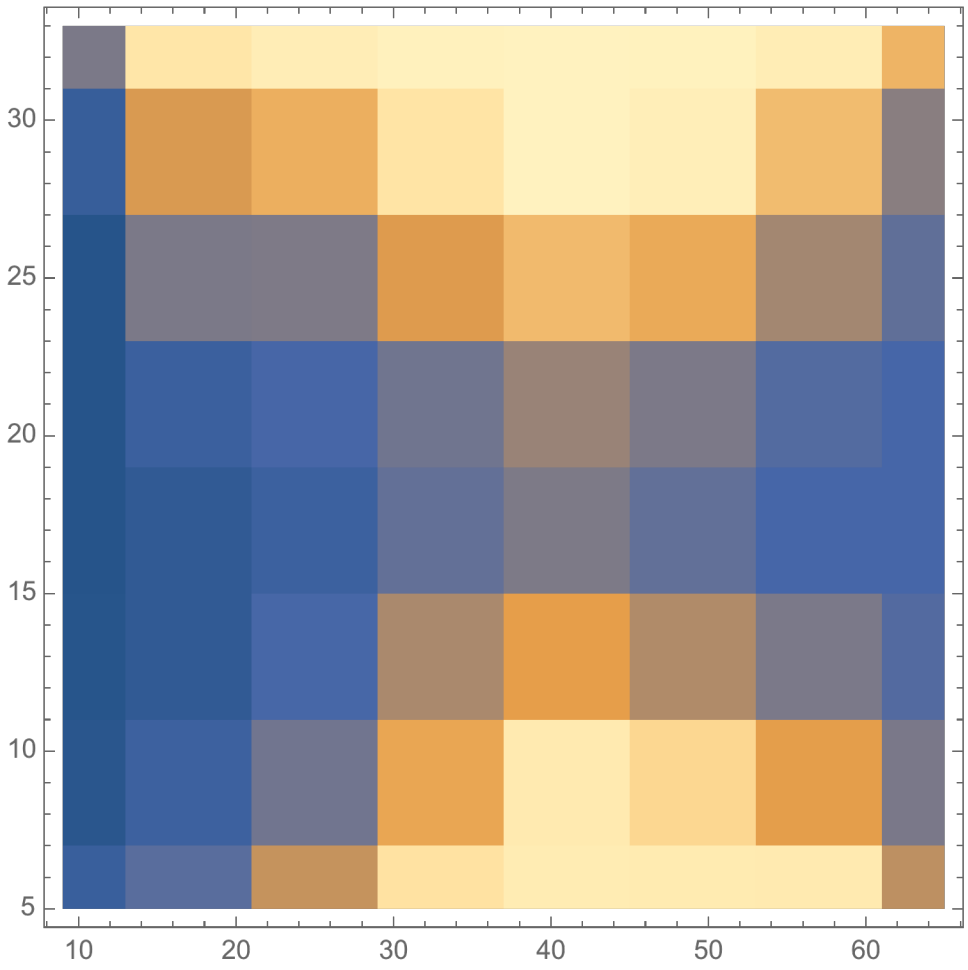

Figure 5.8: Spatial sensitivity when close to tipping towards Snowball Earth. Blue is the most sensitive, and white is the least sensitive

Chapter 6

Early-Warning Signals

Tipping points have potentially significant consequences in many different areas, such as in the financial market, the climate system, and even in psychology [21]. In all of these areas, it is obviously useful to know if a system is a approaching a tipping point.
In this chapter, we will explain what happens as a system approaches a tipping point, and how scientists can detect early warning signals.

6.1 Critical Slow Down

As a dynamical system approaches a bifurcation it is expected to go through critical slow down (CSD): A perturbation or disturbance of a system close to a critical transition will slowly decay back to equilibrium.

CSD can have a number of measurable effects in observational time series. The two most commonly discussed are the increase in variance and the increase in autocorrelation. A number of studies suggest that an increase in autocorrelation is sufficient evidence for EWS [15], though this has been disputed in other studies [22]. The variance can be observed due to a amplification of stochastic fluctuations around the dynamical equilibrium, and the autocorrelation is related to slower response times to stochastic perturbations.

6.1.1 Example of CSD

Marten Scheffer et al. [23] uses an example to show why critical slow down occurs.
Consider the following simple dynamical system, where a and b are parameters, and γ is a positive scaling factor:

$$\frac{dx}{dt} = \gamma(x-a)(x-b) \tag{6.1}$$

This system has two equilibria: $x_1 = a$ and $x_2 = b$. One of these is stable, and the other is unstable. Assuming that x_1 is the stable fixed point, we make a perturbation:

$$x = x_1 + \varepsilon$$

$$\frac{d(x_1+\varepsilon)}{dt} = f(x_1+\varepsilon) \tag{6.2}$$

where $f(x)$ is the right hand side of equation 6.1. Using a first-order Taylor expansion to linearize we obtain

$$\frac{d(x_1+\varepsilon)}{dt} \approx f(x_1) + \left.\frac{\partial f}{\partial x}\right|_{x_1} \varepsilon \tag{6.3}$$

which simplifies to

$$f(x_1) = \frac{d\varepsilon}{dt} = f(x_1) + \left.\frac{\partial f}{\partial x}\right|_{x_1} \varepsilon \Rightarrow \frac{d\varepsilon}{dt} = \lambda\varepsilon \tag{6.4}$$

with eigenvalues λ_1 and λ_2, where

$$\lambda_1 = \left.\frac{\partial f}{\partial x}\right|_a = -\gamma(b-a) \tag{6.5}$$

and for the other fixed point:

$$\lambda_2 = \left.\frac{\partial f}{\partial x}\right|_b = \gamma(b-a) \tag{6.6}$$

From this, it is easy to see that when $b = a$, the recovery rates λ_1 and λ_2 are both zero and the perturbation will not recover. As the system moves away from the bifurcation we can see that the recovery rate in this model is linearly dependent on the size of the basin of attraction, namely $b-a$. This is a very simplistic model, and for more realistic models this is not necessarily true, but the relation is often nearly linear [24].

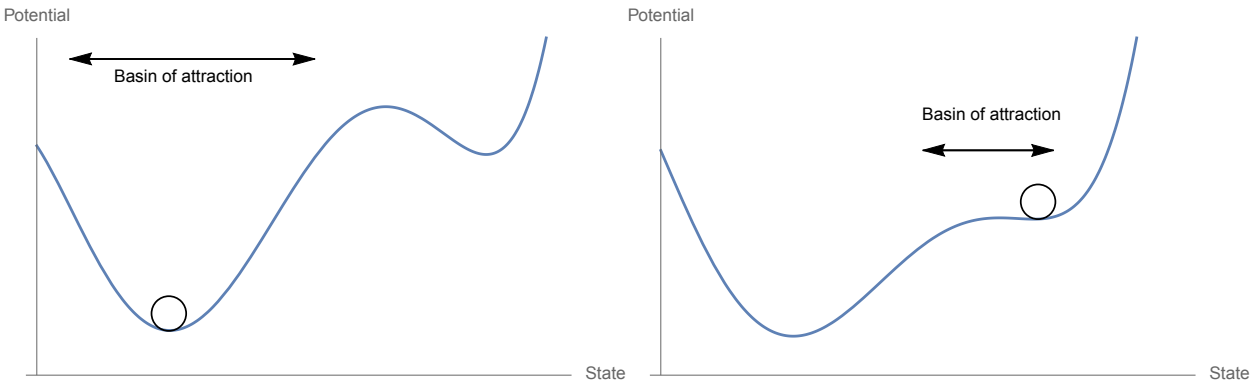

(a) Far from bifurcation

(b) Close to bifurcation

Figure 6.1: (a) The state is far from bifurcation and the basin of attraction is large. This leads to relatively high recovery rate from perturbations. (b) The state is closer to the bifurcation, and the basin of attraction shrinks. The rate of recovery from perturbation is lower

6.1.2 Increased variance and autocorrelation due to CSD

Scheffer et al. [23] also show why CSD can lead to increased variance and autcorrelation.
Consider an autoregressive model of order 1 (AR(1)) on the form

$$y_{n+1} = \alpha y_n + \sigma \varepsilon_n \tag{6.7}$$

where y_n is the deviation of the state variable from the equilibrium, σ is the standard deviation and ε_n is a random number from a standard normal distribution. The autocorrelation is

$$\alpha = e^{\lambda \partial t} \tag{6.8}$$

where ∂t is the time period.
The expectation of an AR(1) process $y_{n+1} = c + \alpha y_n + \sigma \varepsilon_n$ is

$$E(y_{n+1}) = E(c) + \alpha E(y_n) + E(\sigma \varepsilon_n) \Rightarrow \mu = \frac{c}{a - \alpha} \tag{6.9}$$

For $c = 0$, the mean equals zero and the variance is

$$Var(y_{n+1}) = E(y_n)^2 - \mu^2 = \frac{\sigma^2}{1 - \alpha^2} \tag{6.10}$$

Equation 6.8 shows that when λ approaches zero, the autocorrelation tends to one. Because λ approaches zero as the system approaches a bifurcation, a rise in autocorrelation is a valid early warning signal. As the autocorrelation approaches one, the variance tends to infinity. The AR(1) process is the stochastic version of the linearization of the dynamical system. Of course, the linearization is invalid at the bifurcation point, and the variance will remain bounded.

6.2 Other EWS

When a system is close to a TP, we may also have an increase in asymmetry of fluctuations. This asymmetry can lead to skewness [23]. Unlike the increase in variance and autocorrelation, this is not a consequence of CSD, but due to another property of fold bifurcations (Figure 4.1). In the vicinity of an unstable point, the rates of change are lower. This leads to the system spending more time at the unstable region between two potential wells, referred to as the saddle.

Another phenomenon that can be observed is flickering. This is when the stochastic forcing can make the system jump back and forth between two attractors. This happens as a response to a relatively strong noise [25].

6.3 Validity of Early Warning Signals

Even though increasing variance and autocorrelation has been considered a potential indicator of CSD in numerous studies, the exact conditions under which CSD can be deduced from observational time series, are disputed in some recent studies. Some studies demonstrate missed alarms, where an impending critical transition has not been predicted [26], and false alarms, where a critical transition is predicted but never happened [27]. This may be due to a data set ill-suited for CSD detection, or it can be a result of conceptually misunderstanding how CSD is linked to the dynamics of a system.

Bathiany et al. [28] found that EWS for accelerated sea-ice is limited, and their results show that the relaxation time is unrelated to the existence of a tipping point. In some instances, decreasing response times can be explained by other physical processes. For example, a decreased response time during summer sea-ice loss can be caused by thinning of the sea-ice leading to a more efficient heat conduction.

Timothy Lenton [29] suggests two reasons for missed alarms; the first is high noise level. If the noise level is too high, the internal variability of the system is high, and the system can exit its current state before a bifurcation point is reached.
The second reason is if the forcing changes too fast. Existing theory generally assumes a very gradual change in system parameters.
Human activities are forcing certain slow parts of the climate system faster than their internal dynamics allow them to respond. This means that we may not get any warning signals ahead of certain bifurcations in our climate system.

The theory of EWS is based on a very simple example. This may be another problem with the way we currently detect EWS; that they only work for very simplistic models.

Chapter 7

Early-Warning Signals in The Diffusive Energy Balance Model

In this section we will use the concepts explained in Chapter 6 to look for EWS in the model analyzed in this thesis. This means first adding noise to the forcing, and then calculating the change in variance and autocorrelation as the forcing increases or decreases.

7.1 Adding noise to the model

Even though noisy fluctuations can be sufficient to cause a system to undergo an abrupt transition, the noise will usually have to be very strong in order to push the system out of a stable state.

When noise is added to our model we get a combination of a B- and N-tipping, i.e., a noisy linear forcing which forces the system close to a tipping point. The noise may cause the system to tip over earlier or later compared to the case with just a linear forcing. Adding noise to the model changes the partial differential equation we are solving from 3.1 to

$$c\frac{\partial T}{\partial t} = -A - BT + \alpha S + D\nabla^2 T + F + N(t) \tag{7.1}$$

where N is the noise.

The noise added to the the forcing is white noise, created by randomly selecting from a normal distribution $\mathcal{N}(0,\sigma)$, where σ can be adjusted to increase the noise level.

Introducing noise to the model makes it more realistic. The real-world forcing does is not as

shown in Chapter 4. Chaotic weather systems cause fluctuations that force the climate system in a nosy manner.

For each model experiment we made 10 independent runs. The model experiments were set up the same way as described in case 2 in Chapter 4. The results are summarized in Figures 7.1, 7.2, 7.3, and 7.4.

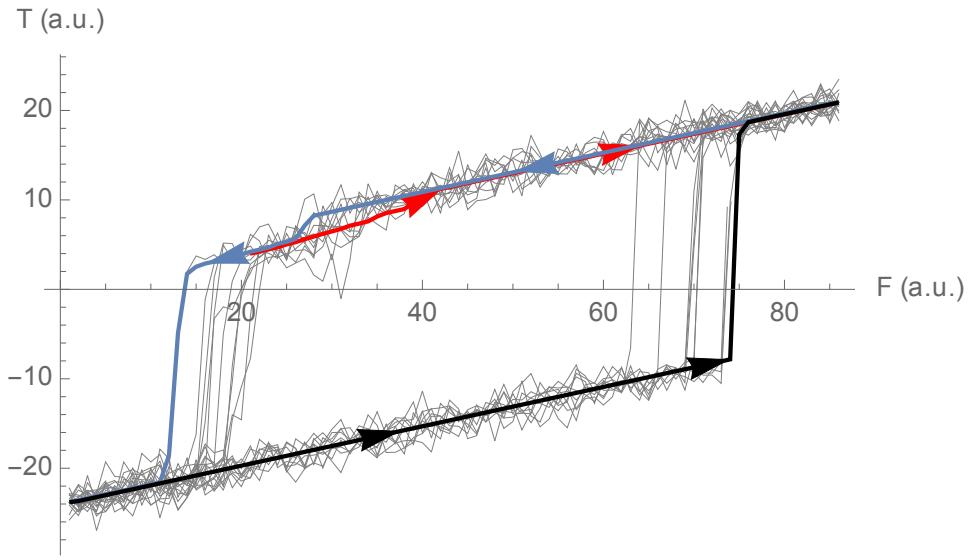

Figure 7.1: Global average temperature response to noisy forcing to and from Snowball Earth

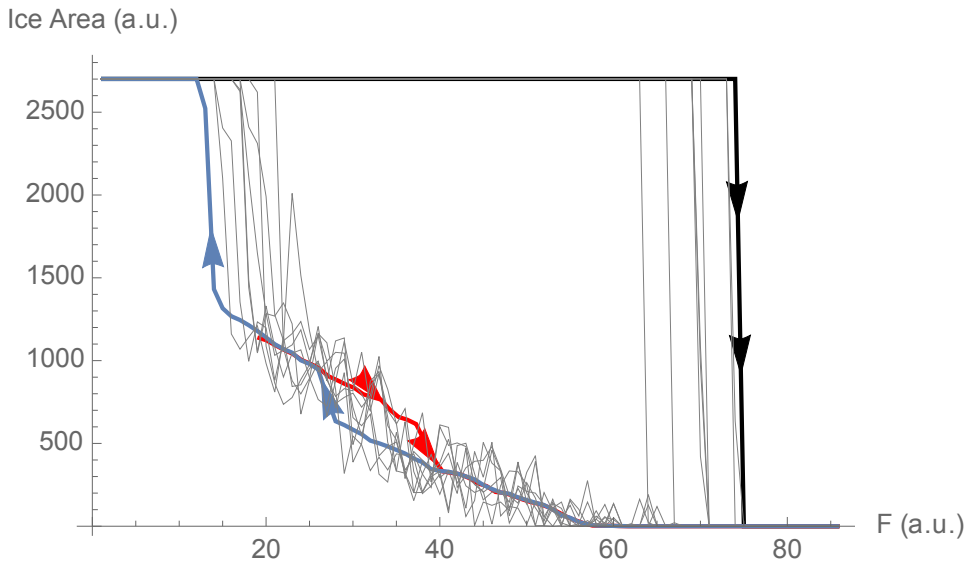

Figure 7.2: Ice area response to noisy forcing to and from Snowball Earth

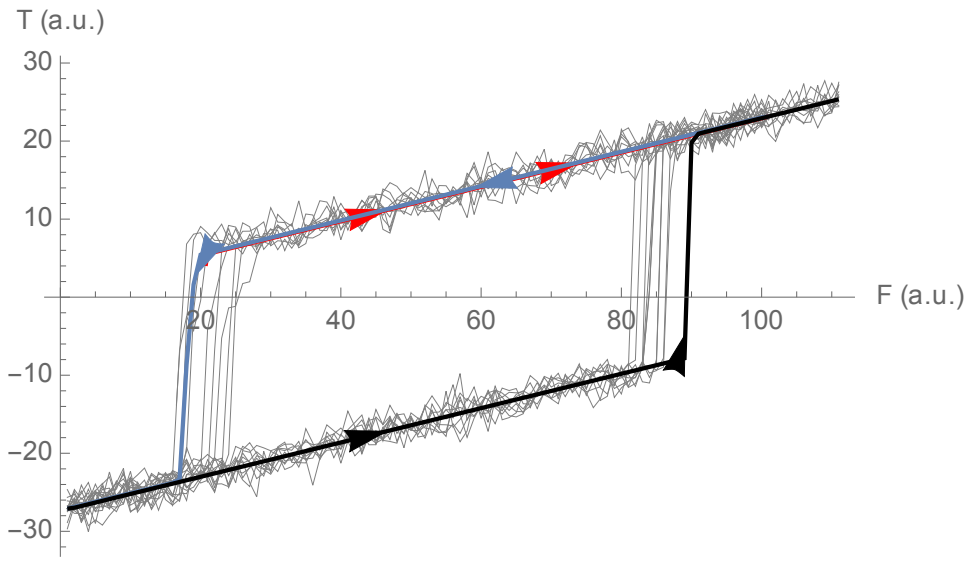

Figure 7.3: Global average temperature response to noisy forcing to and from Snowball Earth without land

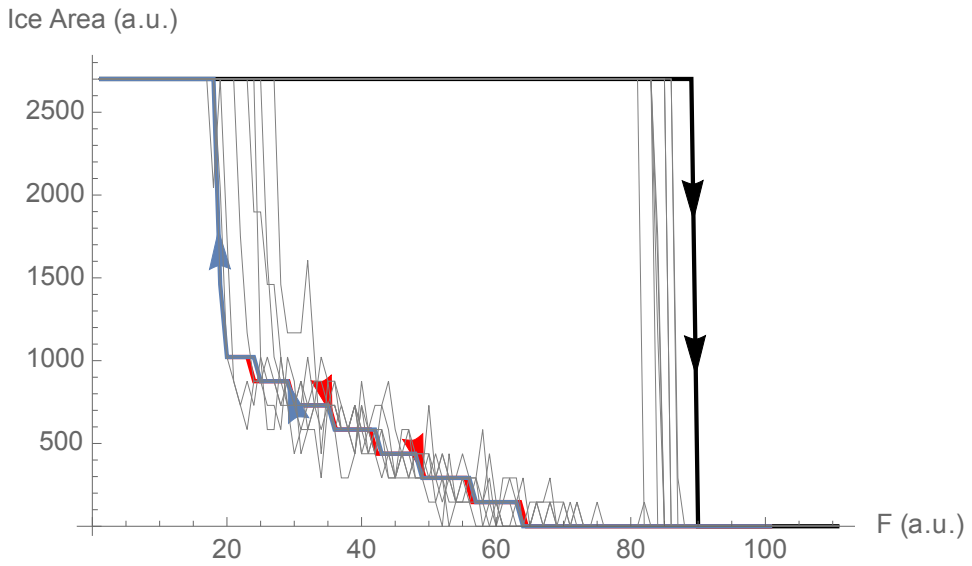

Figure 7.4: Ice area response to noisy forcing to and from Snowball Earth wihout land

This was not done exclusively for Case 1, as it would be included in Case 2.

7.2 Variance and lag-1 correlation

Using the ideas from Chapter 6, we can calculate whether or not there where any warning signals in the runs shown above. Methods for calculating variance and autocorrelation are shown in Appendix B. The variance and autocorrelation were only calculated up until the noisy runs reached the bifurcation point. After the run bifurcates the data is not usable for EWS analysis.

The red lines in the plots are linear regressions of the data points in each plot.

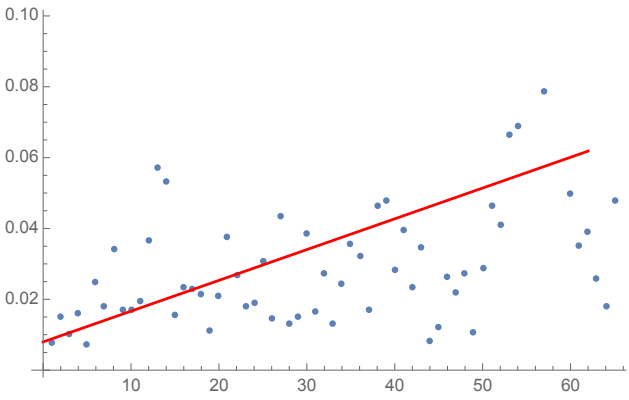

(a) Variance in temperature when forcing towards snowball Earth

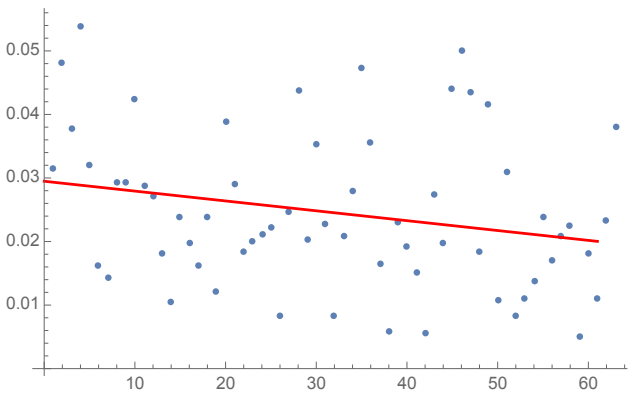

(b) Variance in temperature when forcing from snowball Earth

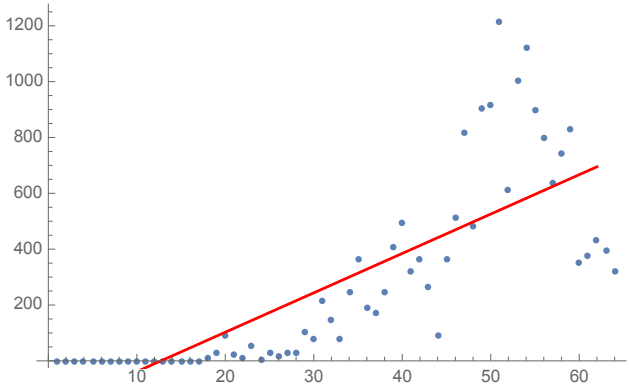

(c) Variance in ice when forcing towards snowball Earth

Figure 7.5: Variance of noisy forcing until bifurcation with land

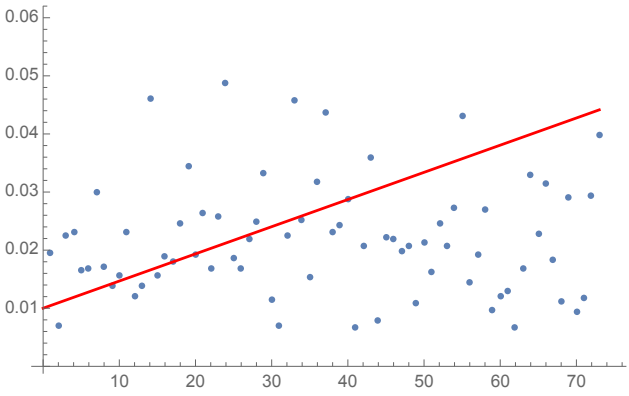

(a) Variance in temperature when forcing towards snowball Earth, no land

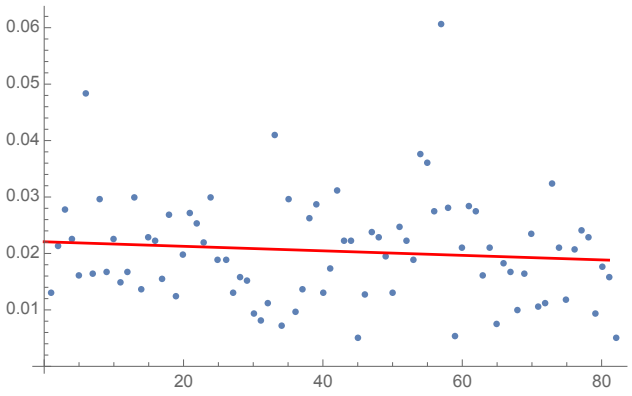

(b) Variance in temperature when forcing from snowball Earth, no land

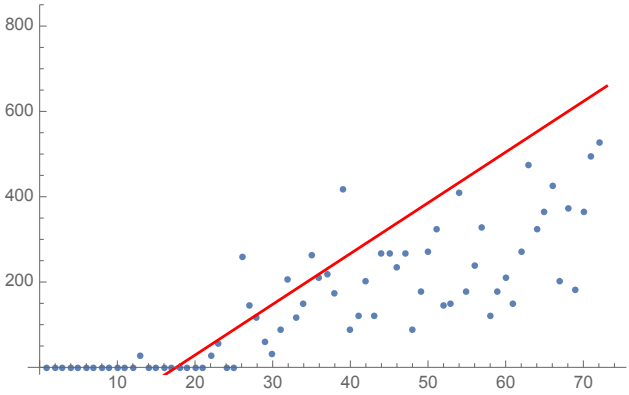

(c) Variance in ice when forcing towards snowball Earth, no land

Figure 7.6: Variance of noisy forcing until bifurcation without land

The variance in ice area when forcing the system out of snowball Earth was zero, meaning there was no difference in the run without noise and runs with noise. This is because in snowball Earth, the entire Earth is covered in ice, and in this model a small perturbation is not enough to melt some of the ice. The only point the perturbation is able to melt some ice, is at the bifurcation point.

Something similar to this happens when we look at the ice area when the system is forced from a warm state towards snowball Earth. When the forcing is very high, and there is no ice on the surface, the noise is not enough to spontaneously form ice.

When the variance is zero, it is not possible to calculate the autocorrelation. Therefore the autocorrelation in ice area when forcing from snowball Earth is not included.

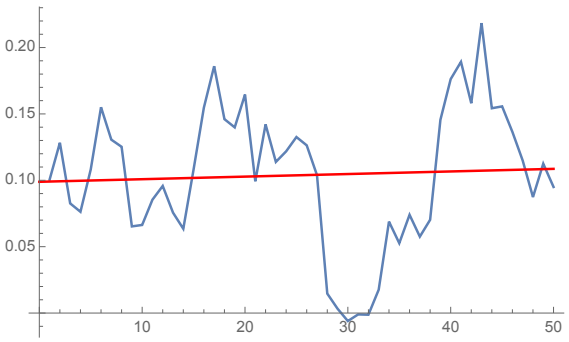

(a) ACF of temperature when forcing towards Snowball Earth

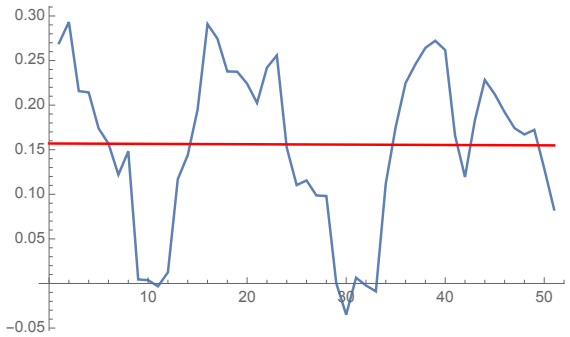

(b) ACF of temperature when forcing from Snowball Earth

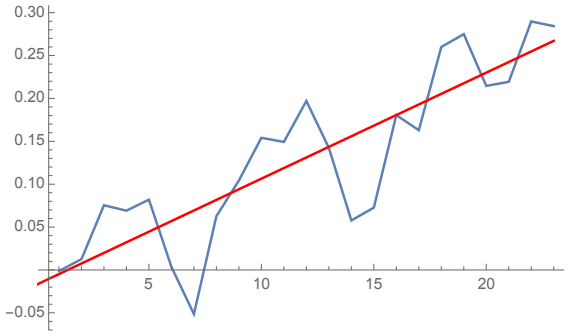

(c) ACF of ice when forcing from Snowball Earth

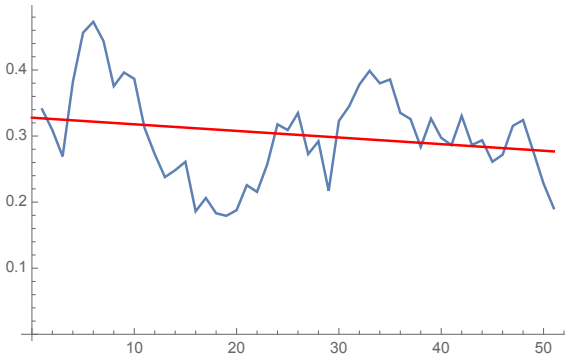

(d) ACF of temperature when forcing towards snowball Earth, no land

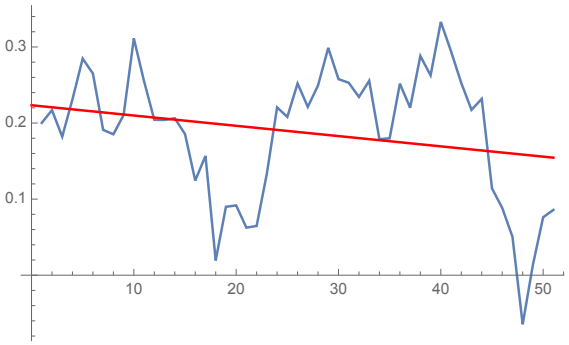

(e) ACF of temperature when forcing from snowball Earth, no land

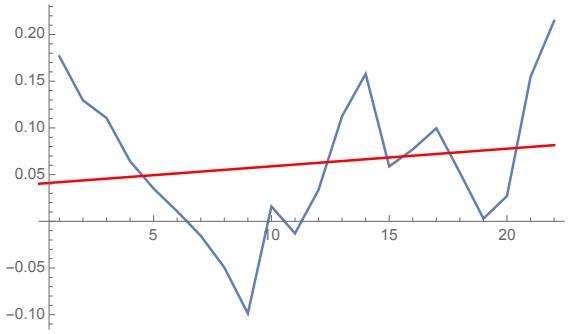

(f) ACF of ice when forcing from snowball Earth, no land

Figure 7.7: ACF of noisy forcing until bifurcation

Chapter 8

Discussion and Analysis

This chapter will elaborate on the results from Chapter 5 and 7.

8.1 The Tipping Points

The tipping points studied in this thesis are in reality very complex phenomena, but the model used is relatively simple. Even though the model produced the two hysteresis loops, it is not sufficient by any means. When the Earth's climate transitions from the snowball state to our current state, it should be able to transition to a climate where there is still ice present on the Earth as shown in Figure 4.2. However, as seen in Figure 5.2 and 5.4, it transitioned directly to a climate warmer than ours and without ice.

We suspect that adding a realistic formation and melting of ice, and couple the model to a deep ocean may help in slowing down this tipping.
In reality the ice does not suddenly disappear when the temperature reaches a given temperature threshold, but that starts the melting process. This would slow down the change in albedo, and therefore also the ice-albedo feedback.
Adding deep ocean to the model would give more realistic values of the thermal inertia of the climate model.

Even though the forcings and temperature used in this thesis are arbitrary units, we can still compare Figure 5.2 and 5.5. The transition from snowball Earth happened at a greater forcing for the run without land than the run with land. This is the same with the transition to snowball Earth. Meaning that the inclusion of land area in this model "shifts" the temperature profile to the left,

relative to the forcing.

8.2 Earth hysteresis loops

The only thing that has changed between Figure 5.2 and 5.5 was the removal of land masses. However, there is a noticeable difference in the hysteresis loops of the two plots. This is evidence that land masses play a big part in forming the second hysteresis loop, between our current climate and one which is warmer and with less ice.

With global warming, the sudden increase in temperatures shown in Figure 5.1 is very interesting. In this model, the jump in temperature happens at the same time as a sudden loss of ice shown in 5.3. The jump in temperature and the loss of ice go hand-in-hand.

Comparing the temperature profiles and their respective ice area profiles, shows a direct link between the two. When the temperature profile had two hysteresis loops, so did the ice area profile, giving an ice area bifurcation. This co-dependency between the ice area and temperature makes the recent loss of Arctic sea-ice even more pertinent.

In the article by Rose and Marshall [20] they found that adding a more complex representation of heat transport resulted in additional bifurcations in the small ice cap instability. We did not observe additional bifurcations with more complex heat transfer alone, but with land area we saw a second hysteresis loop.

8.3 Early warning signals

For most of the cases studied in this thesis, there was some increase in variance as the system approached the tipping point. However, the autocorrelation was not as reliable. Due to there only being 10 realisations in our ensembles, there may not be enough data to draw strong conclusions. Nevertheless we get an idea of the trends. The only time series which saw an increase in both variance and autocorrelation was in ice area when forcing the system away from snowball Earth. This means that this was the only TP in which EWS were detected; the rest are missed alarms.

The second hysteresis loop that occurs when land is included, could be a reason for the missed alarms for the transitions to snowball Earth. Because this is a small TP, the variance and autocorre-

lation can be affected by the small loop that occurs. This cannot be completely ruled out as a cause, but given that we did not observe EWS for the same TP when there was no land, it is unlikely.

As mentioned earlier, one of the reasons for missed alarms could be high noise levels. To account for this, we tested for EWS with different values for the noise level σ (in intervals of 0.5 from 1 to 10). EWS where not observed for any of these values for σ. The rate change in the forcing was also varied.

This leads us to believe that the more complex heat transport may be the cause of these missed alarms.

8.4 Spatial Sensitivity

Figure 5.7 was as we expected it to be. When the planet is entirely covered in ice, the co-albedo is constant. This means that the spatial temperature is only dependent on the incoming radiation from the sun and the transport of heat.

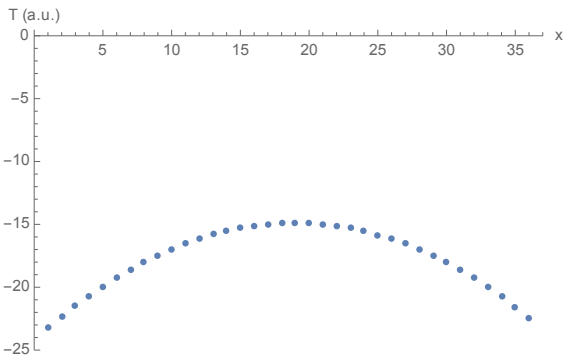

(a) Mean temperature of longitude lines of the Earth in Snowball state

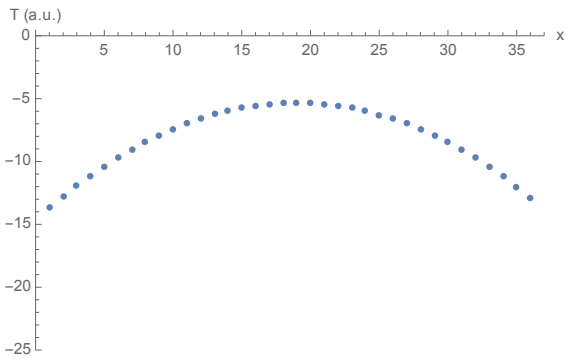

(b) Mean temperature of longitude lines of the Earth in Snowball state when close to TP

Figure 8.1: Temperature response of the Earth to different forcing in Snowball state

The profile of the temperature is the same as long as the climate is in snowball state. As forcing increases or decreases, this curve will just move up and down. This is shown in Figure 8.1, where x is the longitudinal coordinate with $x = 0$ being the North pole and $x = 37$ being the South pole. If the temperature of the equator is increased just slightly, this can lead to a melting of the ice, changing the albedo of this area. This will lead to more energy being absorbed, warming the Earth even more. This will cause a positive feedback effect where ice melting can cause even more ice

to melt. For this to happen at the poles, we need a stronger perturbation than at the equator, since the poles are colder than the equator.

For the transition from snowball Earth we found that the equator is the most sensitive, but it is not always that simple. From Figure 5.7 we see that areas with land masses are more sensitive. It might be this way because ice forms first on land, since the temperature required to form ice on land is higher than in the oceans. The ice-formation will change the albedo and cool the planet even further. Once again, causing a postive feedback loop.

Ideally when looking at spatial sensitivity we want high spatial resolution. This means that the areas perturbed are smaller and the graphics of the result are better. If the areas perturbed become smaller, the size of perturbing must be larger to yield the same effect. This, and the amount of iterations needed to perturb the entire surface of Earth, is very computationally costly. Therefore, the spatial resolution we show here is not very high, but it gives an idea of the spatial sensitivity of the Earth when it is close to a TP.

Chapter 9

Concluding remarks

9.1 Summary

We have shown that including land area is necessary for the global average temperature to have two hysteresis loops in a diffusive EBM. Surprisingly, the transition from snowball Earth ”jumped” to a warmer climate than expected. Nonetheless, this is an interesting result.

We where not able to confidently detect EWS in the cases we tested. One of the reasons for this could be the low number of realizations in our ensembles. It could also be that the model is more complex than the standard models used to demonstrate EWS.

The spatial sensitivity of the Earth when close to a TP showed that generally, the Equator is the most sensitive part. This result was as expected, but still very interesting.

9.2 Further work

Even though the model is dependent on time, the timescale has not been a focus in this thesis. It would be very fascinating to explore how fast these transitions happen, and to see if the introduction of land has changed the speed of the transitions. In this respect, it would also be interesting to couple the model to a deep ocean to get realistic values of the thermal inertia of the climate system.

It would also be very interesting to calculate the spatial sensitivity with higher resolution.

In conclusion, we where able to produce two hysteresis curves, but as explained above, the transi-

tion from snowball Earth was not as we expected. It would be interesting to explore this in more detail.

Appendix A

Implementation of model

A.1 Heat transport on a sphere

The temperature change on a sphere by heat transport is

$$c\frac{\partial T}{\partial t} = D\nabla^2 T$$

where the Laplace operator ∇^2 is defined as

$$\nabla^2 f = \frac{1}{r}\frac{\partial^2}{\partial r^2}(rf) + \frac{1}{r^2\sin\theta}\frac{\partial}{\partial\theta}\left(\sin\theta\frac{\partial f}{\partial\theta}\right) + \frac{1}{r^2\sin^2\theta}\frac{\partial^2 f}{\partial\varphi^2}$$

Here f is a random function, r is the radius of the sphere, θ is the angle of the latitude and φ is the longitudinal angle. Inserting this into the transport equation, we get

$$D\nabla^2 T = D\left[\frac{1}{r}\frac{\partial^2}{\partial r^2}(rT) + \frac{1}{r^2\sin\theta}\frac{\partial}{\partial\theta}\left(\sin\theta\frac{\partial T}{\partial\theta}\right) + \frac{1}{r^2\sin^2\theta}\frac{\partial^2 T}{\partial\varphi^2}\right] \tag{A.1}$$

T is the temperature at sea-level and D is the thermal diffusion coefficient. We also define $x = \cos\theta$ Because we are only looking at the shell of the Earth, there are no changes in r. Therefore $\frac{\partial^2}{\partial r^2} = 0$. We also assume symmetry in longitudinal direction for now, there are no changes in φ.Therefore $\frac{\partial^2}{\partial\varphi^2} = 0$.
For simplicity we also scale the earth so that $r = 1$. Equation A.1 then becomes

$$D\nabla^2 T = D\left[\frac{1}{\sin\theta}\frac{\partial}{\partial\theta}\left(\sin\theta\frac{\partial T}{\partial\theta}\right)\right] \tag{A.2}$$

We start by looking at

$$\frac{1}{\sin\theta}\frac{\partial}{\partial\theta}\left(\sin\theta\frac{\partial T}{\partial\theta}\right)$$

Using the product rule, we get

$$\frac{\partial^2 T}{\partial\theta^2}+\frac{\cos\theta}{\sin\theta}\frac{\partial T}{\partial\theta}$$

By the chain rule, we have

$$\frac{\partial T}{\partial\theta}=\frac{\partial x}{\partial\theta}\frac{\partial T}{\partial x}=\frac{\partial}{\partial\theta}(\cos\theta)\frac{\partial T}{\partial x}=-\sin\theta\frac{\partial T}{\partial x}$$

$$\frac{\partial^2 T}{\partial\theta^2}=\frac{\partial^2 T}{\partial x^2}\left(\frac{\partial x}{\partial\theta}\right)^2+\frac{\partial T}{\partial x}\frac{\partial^2 x}{\partial\theta^2}=\frac{\partial^2 T}{\partial x^2}\sin^2\theta-\cos\theta\frac{\partial T}{\partial x}$$

This means that the right hand side of equation A.2 is now

$$D\left[\sin^2\theta\frac{\partial^2 T}{\partial x^2}-\cos\theta\frac{\partial T}{\partial x}-\sin\theta\frac{\cos\theta}{\sin\theta}\frac{\partial T}{\partial x}\right]$$

$$D\left[\sin^2\theta\frac{\partial^2 T}{\partial x^2}-2\cos\theta\frac{\partial T}{\partial x}\right]$$

Now we can use $x=\cos\theta$ which means that $\sin\theta=\sqrt{1-x^2}$.

$$D\nabla^2 T=D\left[-2x\frac{dT}{dx}+(1-x^2)\frac{d^2T}{dx^2}\right] \tag{A.3}$$

Now we discretize x, we choose a uniform grid $x_i, 0\leq i\leq n$ with spacing $\Delta x=1/n$ such that $x_i=-1+2i\Delta x$. The reason for defining x_i in such a way, is to have $x_i\in[-1,1]$ This means that T is now $T(x_i,t)$
We can approximate $\frac{\partial T_i}{\partial x_i}$ and $\frac{\partial^2 T_i}{\partial x_i^2}$ using centered difference. The first order derivative is then

$$\frac{\partial T_i}{\partial x_i}\approx\frac{T_{i+1}-T_{i-1}}{2\Delta x}$$

and the second-order derivative is

$$\frac{\partial^2 T_i}{\partial x_i^2}\approx\frac{T_{i+1}-2T_i+T_{i-1}}{\Delta x^2}$$

The right hand side of equation A.3 is then

$$D\left[-x_i\frac{T_{i+1}-T_{i-1}}{\Delta x}+(1-x_i^2)\frac{T_{i+1}-2T_i+T_{i-1}}{\Delta x^2}\right]$$

$$D\left[\left(\frac{x_i}{\Delta x}+\frac{1-x_i^2}{\Delta x^2}\right)T_{i-1}-2\left(\frac{1-x_i^2}{\Delta x^2}\right)T_i+\left(-\frac{x_i}{\Delta x}+\frac{1-x_i^2}{\Delta x^2}\right)T_{i+1}\right]$$

We now look at heat transport along the longitudinal direction, therefore $\frac{\partial^2}{\partial\varphi^2}\neq 0$ we have

$$D\nabla^2 T = D\left[\frac{1}{\sin\theta}\frac{\partial}{\partial\theta}\left(\sin\theta\frac{\partial T}{\partial\theta}\right)+\frac{1}{\sin^2\theta}\frac{\partial^2 T}{\partial\varphi^2}\right] \tag{A.4}$$

So we need to take a look at

$$\frac{1}{\sin^2\theta}\frac{\partial^2 T}{\partial\varphi^2} \tag{A.5}$$

We start by defining $y=\varphi$, the we simply have

$$\frac{1}{1-x^2}\frac{\partial^2 T}{\partial y^2}$$

Now we discretize y, we choose a uniform grid $y_j, 0\leq j\leq 2\pi$ with spacing $\Delta y = 1/m$ such that $y_j = 2\pi\Delta y$. The reason for defining y_j in such a way, is to have it go around the equator and come back to the same point it started at. We can approximate $\frac{\partial^2 T_j}{\partial y_j^2}$ using centered difference.

$$\frac{\partial^2 T_j}{\partial y_j^2}\approx\frac{T_{j+1}-2T_j+T_{j-1}}{\Delta y^2}$$

Then equation A.4 becomes

$$D\left[\left(\frac{x_i}{\Delta x}+\frac{1-x_i^2}{\Delta x^2}\right)T_{i-1,j}-2\left(\frac{1-x_i^2}{\Delta x^2}\right)T_{i,j}\right. \tag{A.6}$$

$$\left.+\left(-\frac{x_i}{\Delta x}+\frac{1-x_i^2}{\Delta x^2}\right)T_{i+1,j}+\left(\frac{1}{1-x_i^2}\right)\frac{T_{i,j+1}-2T_{i,j}+T_{i,j-1}}{\Delta y^2}\right]$$

A.2 Area of a grid cell

The area between a line of lattitude and the North Pole is

$$A = 2\pi \cdot R \cdot h \tag{A.7}$$

where R is the radius og the Earth an h is the perpendicular distance plane containing the line of latitude to the pole.

$$h = R(1 - \sin lat)$$

Inserting this into A.7 gives us

$$A = 2\pi \cdot R^2(1 - \sin\theta) \tag{A.8}$$

The area between to lines of latitude is therefore

$$A = 2\pi \cdot R^2|\sin\theta_1 - \sin\theta_2| \tag{A.9}$$

The area of a latitude longitude rectangle is proportional to the difference in longitudes. Therefore the area we seek is

$$A = 2\pi \cdot R^2|\sin\theta_1 - \sin\theta_2||\varphi_1 - \varphi_2|/360$$

$$A = \frac{\pi}{180} \cdot R^2|\sin\theta_1 - \sin\theta_2||\varphi_1 - \varphi_2| \tag{A.10}$$

Using that $\theta = \sqrt{1 - x_i}$ and $\varphi = y_i$ this equation becomes

$$A_{i,j} = \frac{\pi}{180}R^2|\sqrt{1 - x_i^2} - \sqrt{1 - x_{i+1}^2}|\cdot|y_j - y_{j+1}|$$

Appendix B

Calculating σ^2 and ρ

The variance σ^2 is simply the square of the ensemble member subtracted from the run without noise.

$$\sigma^2 = \frac{1}{N}\sum_{i=0}^{N-1}(X_i - \bar{X})^2 \tag{B.1}$$

where N is the ensemble size, X_i is the ensemble member and $\bar{X}$ is the run without noise.

Autocorrelation function ρ is the correlation between two lag 1 offset windows of the time series.

$$\rho = \frac{1}{N-1}\sum_{j=1}^{j-1}\frac{(X_{j,i,1} - \mu)(X_{j,i,2} - \mu)}{\sigma^2} \tag{B.2}$$

where $X_{j,i,1} = [x_{j,i+1}, \ldots, x_{j,i+p}]$, $X_{j,i,2} = [x_{j,i}, \ldots, x_{j,i+p-1}]$, x_j is the ensemble member j, p is the length of the window and μ is the mean.

Appendix C

Mathematica code

Importing a map of the Earth

```
δ = 5;
data = GeoElevationData[
   GeoPosition[Table[{lat, lon}, {lat, -90, 90, δ}, {lon, 0, 360, δ}]]];
data2 = Map[UnitStep[#[[1]]] &, Flatten[data]];
data2 = Partition[data2, Dimensions[data][[2]]];

(*For aquaplanet run this cell*)
(*data2={};
Do[
data2=Append[data2,0]
,{i,0,2701}];
data2=Partition[data2,m];*)
```

Defining parameters

```
n = Dimensions[data2][[1]] - 1;
m = Dimensions[data2][[2]];
A = 200.;
B = 1 / 0.22;
d = 0.38;
s2 = -0.482;
b0 = 0.38;
a0 = 0.697;
a2 = -0.0779;
Q = 334.4;
cc = 1;
q = 10;
US = (1 + Tanh[q #]) / 2 & ;
d = 0.5 + 0.0125 * Flatten[data2];

M = (n + 1) * m;
Δx = 1. / n;
x = Table[-1. + 2 i / n, {i, 0, n}];
S = Table[1 + s2 * LegendreP[2, x], {m}];
F = Table[Sign[-1. + 2 i / n], {i, 0, n}];
F = Flatten[Transpose[Table[F, {m}]]];
F2 = Table[1, {i, 0, n}];
F2 = Flatten[Transpose[Table[F2, {m}]]];
x = Flatten[Transpose[Table[x, {m}]]];
Δy = N[2 π / m];
y = Table[N[2 π i / m], {i, 0, m - 1}];
S = Flatten[Transpose[S]];
R = 0.7 * Flatten[data2] + 0.8 * (1 - Flatten[data2]) ^ 2;
Tc = (-3) * Flatten[data2] + (-5) * (1 - Flatten[data2]) ^ 2;
a = x / Δx + (1 - x ^ 2) / Δx ^ 2;
b = -2 (1 - x ^ 2) / Δx ^ 2;
c = -x / Δx + (1 - x ^ 2) / Δx ^ 2;
plus1[tall_] := (
  If[Mod[tall, m] == 0,
    Return[tall - (m - 1)];,
    Return[tall + 1];
   ];
 )
minus1[tall_] := (
  If[Mod[tall - 1, m] == 0,
    Return[tall + (m - 1)];,
    Return[tall - 1];
   ];
 )
```

Calculating the Area of each grid cell

```
Areal
Δ1 = 1;
imax = Dimensions[data2][[1]];
jmax = Dimensions[data2][[2]];
A1 = Table[
   Abs[Sqrt[1 - ((i - Δ1) * Δx)^2] - Sqrt[1 - ((i + Δ1) * Δx)^2]], {i, 1, imax / 2}];
A2 = Reverse[A1];
A3 = Join[A1, A2];
A3 = A3 / Max[A3];
Do[
 A3[[i]] = A3[[i]] - 0.07777 * A3[[i]]
 , {i, 1, 36, 1}]
A3 = Insert[A3, 1, 19];
ListPlot[A3]
```

Creating a list where temperature of grid cells can be entered

```
Tliste = Table[ToExpression[
    StringJoin[StringJoin[ToString[T], ToString[i]], "[t]"]], {i, 1, M}];
```

Implementing the model

```
firsteq =
  Table[cc * D[Tliste[[i]], t] == d[[i]] * 2 * (Tliste[[i + m]] - Tliste[[i]]) / Δx +
     Q S[[i]] * (b0 * US[Tc[[i]] - Tliste[[i]]] + R[[i]] * US[Tliste[[i]] - Tc[[i]]]) +
     (-A - B Tliste[[i]]), {i, 1, m}];
lasteq = Table[cc * D[Tliste[[i]], t] ==
    d[[i]] * (-2) * (Tliste[[i]] - Tliste[[i - m]]) / Δx +
     Q S[[i]] * (b0 * US[Tc[[i]] - Tliste[[i]]] + R[[i]] * US[Tliste[[i]] - Tc[[i]]]) +
     (-A - B Tliste[[i]]), {i, n * m + 1, n * m + m}];
eqliste = Table[
   cc * D[Tliste[[i]], t] ==
    d[[i]] * (Simplify[a[[i]] * Tliste[[i - m]] + b[[i]] * Tliste[[i]] +
          c[[i]] * Tliste[[i + m]]] + 1 / (Δy^2 * (1 - x[[i]]^2)) *
         (Tliste[[plus1[i]]] - 2 Tliste[[i]] + Tliste[[minus1[i]]])) +
     Q S[[i]] * (b0 * US[Tc[[i]] - Tliste[[i]]] + R[[i]] * US[Tliste[[i]] - Tc[[i]]]) +
     (-A - B Tliste[[i]])
   , {i, m + 1, m * n}];
eqliste = Join[firsteq, eqliste, lasteq];
X = Table[-1. + 2 i / n, {i, 0, n}];
Y = Table[2 π i / m, {i, 0, m - 1}];
```

Setting a symmetric starting value of the temperatures, the starting temperature will define which of the stable states
the model will start in.

```
X = Table[-1. + 2 i / n, {i, 0, n}];
Y = Table[2 π i / m, {i, 0, m - 1}];
startliste = Table[ToExpression[
    StringJoin[StringJoin[ToString[T], ToString[i]], "[0]"]], {i, 1, M}];
startverdier = Flatten[5 + Table[Exp[-X[[ii]]^2] * (1 + 0.5 * Sin[Y[[jj]]]),
     {ii, 1, n + 1}, {jj, 1, m}]];
start = Table[startliste[[i]] == startverdier[[i]], {i, 1, M}];
```

Defining the forcing to change with time t, and creating a nested look that gives the temperature in each grid cell at each time step t. This forcing can be changed to get different forcing like negative or bigger forcing

Running the model

In this run we are forcing the system from the initial values to close to the tipping point towards snowball Earth

In[•]:=
```
f = t;
```

In[•]:=
```
firsteq =
  Table[cc * D[Tliste[[i]], t] == d[[i]] * 2 * (Tliste[[i + m]] - Tliste[[i]]) / Δx +
     Q S[[i]] * (b0 * US[Tc[[i]] - Tliste[[i]]] + R[[i]] * US[Tliste[[i]] - Tc[[i]]]) +
     (-A - B Tliste[[i]]) - f, {i, 1, m}];
lasteq = Table[cc * D[Tliste[[i]], t] ==
    d[[i]] * (-2) * (Tliste[[i]] - Tliste[[i - m]]) / Δx +
     Q S[[i]] * (b0 * US[Tc[[i]] - Tliste[[i]]] + R[[i]] * US[Tliste[[i]] - Tc[[i]]]) +
     (-A - B Tliste[[i]]) - f, {i, n * m + 1, n * m + m}];
eqliste = Table[
   cc * D[Tliste[[i]], t] ==
    d[[i]] * (Simplify[a[[i]] * Tliste[[i - m]] + b[[i]] * Tliste[[i]] +
          c[[i]] * Tliste[[i + m]]] + 1 / (Δy^2 * (1 - x[[i]]^2)) *
         (Tliste[[plus1[i]]] - 2 Tliste[[i]] + Tliste[[minus1[i]]])) +
     Q S[[i]] * (b0 * US[Tc[[i]] - Tliste[[i]]] + R[[i]] * US[Tliste[[i]] - Tc[[i]]]) +
     (-A - B Tliste[[i]]) - f
   , {i, m + 1, m * n}];
eqliste = Join[firsteq, eqliste, lasteq];
```

In[•]:=
```
Timing[
 sol = NDSolve[Join[eqliste, start], Tliste, {t, 0, 6}];
]
```

In[•]:=
```
løsning1 = Table[(Evaluate[Tliste /. sol] /. t → tt)[[1]], {tt, 0, 6, 1}];
```

Starting form where the last run ended, we increase the forcing to warm up the Earth past the starting point

In[•]:=
```
startfromtp = Table[startliste[[i]] == Last[løsning1][[i]], {i, 1, M}];
f = -6 + t;
```

```
In[•]:=
firsteq =
  Table[cc * D[Tliste[[i]], t] == d[[i]] * 2 * (Tliste[[i + m]] - Tliste[[i]]) / Δx +
     Q S[[i]] * (b0 * US[Tc[[i]] - Tliste[[i]]] + R[[i]] * US[Tliste[[i]] - Tc[[i]]]) +
     (-A - B Tliste[[i]]) + f, {i, 1, m}];
lasteq = Table[cc * D[Tliste[[i]], t] ==
    d[[i]] * (-2) * (Tliste[[i]] - Tliste[[i - m]]) / Δx +
     Q S[[i]] * (b0 * US[Tc[[i]] - Tliste[[i]]] + R[[i]] * US[Tliste[[i]] - Tc[[i]]]) +
     (-A - B Tliste[[i]]) + f, {i, n * m + 1, n * m + m}];
eqliste = Table[
   cc * D[Tliste[[i]], t] ==
    d[[i]] * (Simplify[a[[i]] * Tliste[[i - m]] + b[[i]] * Tliste[[i]] +
          c[[i]] * Tliste[[i + m]]] + 1 / (Δy^2 * (1 - x[[i]]^2)) *
         (Tliste[[plus1[i]]] - 2 Tliste[[i]] + Tliste[[minus1[i]]])) +
     Q S[[i]] * (b0 * US[Tc[[i]] - Tliste[[i]]] + R[[i]] * US[Tliste[[i]] - Tc[[i]]]) +
     (-A - B Tliste[[i]]) + f
   , {i, m + 1, m * n}];
eqliste = Join[firsteq, eqliste, lasteq];

In[•]:= Timing[
 sol = NDSolve[Join[eqliste, startfromtp], Tliste, {t, 0, 66}];
]

In[•]:= løsning2 = Table[(Evaluate[Tliste /. sol] /. t → tt)[[1]], {tt, 0, 66, 1}];
```

Starting from where the last run ended, we decrease the forcing to cool the Earth down to snowball Earth

```
In[•]:= startfromwarm = Table[startliste[[i]] == Last[løsning2][[i]], {i, 1, M}];
f = -60 + t;
```

```
In[•]:= firsteq =
          Table[cc * D[Tliste[[i]], t] == d[[i]] * 2 * (Tliste[[i + m]] - Tliste[[i]]) / Δx +
              Q S[[i]] * (b0 * US[Tc[[i]] - Tliste[[i]]] + R[[i]] * US[Tliste[[i]] - Tc[[i]]]) +
              (-A - B Tliste[[i]]) - f, {i, 1, m}];
        lasteq = Table[cc * D[Tliste[[i]], t] ==
             d[[i]] * (-2) * (Tliste[[i]] - Tliste[[i - m]]) / Δx +
              Q S[[i]] * (b0 * US[Tc[[i]] - Tliste[[i]]] + R[[i]] * US[Tliste[[i]] - Tc[[i]]]) +
              (-A - B Tliste[[i]]) - f, {i, n * m + 1, n * m + m}];
        eqliste = Table[
            cc * D[Tliste[[i]], t] ==
             d[[i]] * (Simplify[a[[i]] * Tliste[[i - m]] + b[[i]] * Tliste[[i]] +
                    c[[i]] * Tliste[[i + m]]] + 1 / (Δy^2 * (1 - x[[i]]^2)) *
                  (Tliste[[plus1[i]]] - 2 Tliste[[i]] + Tliste[[minus1[i]]])) +
              Q S[[i]] * (b0 * US[Tc[[i]] - Tliste[[i]]] + R[[i]] * US[Tliste[[i]] - Tc[[i]]]) +
              (-A - B Tliste[[i]]) - f
            , {i, m + 1, m * n}];
        eqliste = Join[firsteq, eqliste, lasteq];

In[•]:= Timing[
         sol = NDSolve[Join[eqliste, startfromwarm], Tliste, {t, 0, 85}];
        ]


In[•]:= løsning3 = Table[(Evaluate[Tliste /. sol] /. t → tt)[[1]], {tt, 0, 85, 1}];
```

Starting from where the last run ended, we increase the forcing to warm the Earth out of Snowball Earth

```
In[•]:= startfromcold = Table[startliste[[i]] == Last[løsning3][[i]], {i, 1, M}];
        fwarming = -25 + t;

In[•]:= firsteq =
          Table[cc * D[Tliste[[i]], t] == d[[i]] * 2 * (Tliste[[i + m]] - Tliste[[i]]) / Δx +
              Q S[[i]] * (b0 * US[Tc[[i]] - Tliste[[i]]] + R[[i]] * US[Tliste[[i]] - Tc[[i]]]) +
              (-A - B Tliste[[i]]) + fwarming, {i, 1, m}];
        lasteq = Table[cc * D[Tliste[[i]], t] ==
             d[[i]] * (-2) * (Tliste[[i]] - Tliste[[i - m]]) / Δx +
              Q S[[i]] * (b0 * US[Tc[[i]] - Tliste[[i]]] + R[[i]] * US[Tliste[[i]] - Tc[[i]]]) +
              (-A - B Tliste[[i]]) + fwarming, {i, n * m + 1, n * m + m}];
        eqliste = Table[
            cc * D[Tliste[[i]], t] ==
             d[[i]] * (Simplify[a[[i]] * Tliste[[i - m]] + b[[i]] * Tliste[[i]] +
                    c[[i]] * Tliste[[i + m]]] + 1 / (Δy^2 * (1 - x[[i]]^2)) *
                  (Tliste[[plus1[i]]] - 2 Tliste[[i]] + Tliste[[minus1[i]]])) +
              Q S[[i]] * (b0 * US[Tc[[i]] - Tliste[[i]]] + R[[i]] * US[Tliste[[i]] - Tc[[i]]]) +
              (-A - B Tliste[[i]]) + fwarming
            , {i, m + 1, m * n}];
        eqliste = Join[firsteq, eqliste, lasteq];
```

```
In[•]:= Timing[
         sol = NDSolve[Join[eqliste, startfromcold], Tliste, {t, 0, 85}];
        ]
```

```
In[•]:=
```

```
løsning4 = Table[(Evaluate[Tliste /. sol] /. t → tt)[[1]], {tt, 0, 85, 1}];
```

Creating lists of the average global temperature change with time in the runs above

```
gjennom = {};
Do[
  mean = Mean[løsning2[[i]]];
  gjennom = Append[gjennom, mean];
  , {i, 1, Length[løsning2]}];

gjennom2 = {};
Do[
  mean2 = Mean[løsning3[[i]]];
  gjennom2 = Prepend[gjennom2, mean2];
  , {i, 1, Length[løsning3]}];


gjennom3 = {};
Do[
  mean3 = Mean[løsning4[[i]]];
  gjennom3 = Append[gjennom3, mean3];
  , {i, 1, Length[løsning4]}];
length = Length[gjennom2] - Length[gjennom];
Do[
  gjennom = Prepend[gjennom, 0];
  , {i, 1, Length[gjennom2] - Length[gjennom]}];
```

Calculating the Ice Area in each of the runs above

```
ice = {};
icearea = {};
Do[
  tempice = UnitStep[løsning2[[i, All]] + Tc];
  ice = Append[ice, tempice];
  , {i, 1, Length[løsning2]}];

Do[
  icearea = Prepend[icearea, Total[ice[[i]]]];
  , {i, 1, Length[løsning2]}];

ice1 = {};
icearea1 = {};

Do[
  tempice1 = UnitStep[løsning3[[i, All]] + Tc];
  ice1 = Append[ice1, tempice1];
  , {i, 1, Length[løsning3]}];

Do[
  icearea1 = Append[icearea1, Total[ice1[[i]]]];
  , {i, 1, Length[løsning3]}];

ice2 = {};
icearea2 = {};

Do[
  tempice2 = UnitStep[løsning4[[i, All]] + Tc];
  ice2 = Append[ice2, tempice2];
  , {i, 1, Length[løsning4]}];

Do[
  icearea2 = Prepend[icearea2, Total[ice2[[i]]]];
  , {i, 1, Length[løsning4]}];
```

Creating noisy run

Creating noise as a function of t

```
sigma = 7;
noise = Interpolation[
   Table[{t, RandomReal[NormalDistribution[0, sigma]]}, {t, -1, 100}]];
```

Noisy forcing from warm state to snowball Earth, by running the above cell we get a new noise function and the noisy run can be done again.

```
startfromwarm = Table[startliste[[i]] == Last[løsning2][[i]], {i, 1, M}];
f = -60 + t + noise[t];
firsteq =
  Table[cc * D[Tliste[[i]], t] == d[[i]] * 2 * (Tliste[[i + m]] - Tliste[[i]]) / Δx +
     Q S[[i]] * (b0 * US[Tc[[i]] - Tliste[[i]]] + R[[i]] * US[Tliste[[i]] - Tc[[i]]]) +
     (-A - B Tliste[[i]]) - f, {i, 1, m}];
lasteq = Table[cc * D[Tliste[[i]], t] ==
    d[[i]] * (-2) * (Tliste[[i]] - Tliste[[i - m]]) / Δx +
     Q S[[i]] * (b0 * US[Tc[[i]] - Tliste[[i]]] + R[[i]] * US[Tliste[[i]] - Tc[[i]]]) +
     (-A - B Tliste[[i]]) - f, {i, n * m + 1, n * m + m}];
eqliste = Table[
   cc * D[Tliste[[i]], t] ==
    d[[i]] * (Simplify[a[[i]] * Tliste[[i - m]] + b[[i]] * Tliste[[i]] +
          c[[i]] * Tliste[[i + m]]] + 1 / (Δy^2 * (1 - x[[i]]^2)) *
         (Tliste[[plus1[i]]] - 2 Tliste[[i]] + Tliste[[minus1[i]]])) +
     Q S[[i]] * (b0 * US[Tc[[i]] - Tliste[[i]]] + R[[i]] * US[Tliste[[i]] - Tc[[i]]]) +
     (-A - B Tliste[[i]]) - f
   , {i, m + 1, m * n}];
eqliste = Join[firsteq, eqliste, lasteq];
Timing[
 sol = NDSolve[Join[eqliste, startfromwarm], Tliste, {t, 0, 100}];
]
løsning3 = Table[(Evaluate[Tliste /. sol] /. t → tt)[[1]], {tt, 0, 100, 1}];
```

Noisy run from Snowball Earth to a warm state

```
startfromcold = Table[startliste[[i]] == Last[løsning3][[i]], {i, 1, M}];
fwarming = -40 + t + noise[t];
firsteq =
  Table[cc * D[Tliste[[i]], t] == d[[i]] * 2 * (Tliste[[i + m]] - Tliste[[i]]) / Δx +
     Q S[[i]] * (b0 * US[Tc[[i]] - Tliste[[i]]] + R[[i]] * US[Tliste[[i]] - Tc[[i]]]) +
     (-A - B Tliste[[i]]) + fwarming, {i, 1, m}];
lasteq = Table[cc * D[Tliste[[i]], t] ==
    d[[i]] * (-2) * (Tliste[[i]] - Tliste[[i - m]]) / Δx +
     Q S[[i]] * (b0 * US[Tc[[i]] - Tliste[[i]]] + R[[i]] * US[Tliste[[i]] - Tc[[i]]]) +
     (-A - B Tliste[[i]]) + fwarming, {i, n * m + 1, n * m + m}];
eqliste = Table[
   cc * D[Tliste[[i]], t] ==
    d[[i]] * (Simplify[a[[i]] * Tliste[[i - m]] + b[[i]] * Tliste[[i]] +
          c[[i]] * Tliste[[i + m]]] + 1 / (Δy^2 * (1 - x[[i]]^2)) *
         (Tliste[[plus1[i]]] - 2 Tliste[[i]] + Tliste[[minus1[i]]])) +
     Q S[[i]] * (b0 * US[Tc[[i]] - Tliste[[i]]] + R[[i]] * US[Tliste[[i]] - Tc[[i]]]) +
     (-A - B Tliste[[i]]) + fwarming
   , {i, m + 1, m * n}];
eqliste = Join[firsteq, eqliste, lasteq];
Timing[
 sol = NDSolve[Join[eqliste, startfromcold], Tliste, {t, 0, 110}];
]
løsning4 = Table[(Evaluate[Tliste /. sol] /. t → tt)[[1]], {tt, 0, 110, 1}];
```

Var and Autocorrrelation

The mathematical methods for this section can be found in appendix B in the thesis

After simulating a noisy run the variance of these runs can be calculated using the cell below, where Warmtosnowball is the run without noise

```
In[•]:= var11 = {};
Do[
  vartemp11 = (1 / Length[EWSto1]) * (EWSto1[[i]] - Warmtosnowball[[i]])^2;
  var11 = Append[var11, vartemp11];
  , {i, 1, Length[EWSto1]}];
var12 = {};
Do[
  vartemp12 = (1 / Length[EWSto2]) * (EWSto2[[i]] - Warmtosnowball[[i]])^2;
  var12 = Append[var12, vartemp12];
  , {i, 1, Length[EWSto2]}];
var13 = {};
Do[
  vartemp13 = (1 / Length[EWSto3]) * (EWSto3[[i]] - Warmtosnowball[[i]])^2;
  var13 = Append[var13, vartemp13];
  , {i, 1, Length[EWSto3]}];
var14 = {};
```

```
Do[
  vartemp14 = (1 / Length[EWSto4]) * (EWSto4[[i]] - Warmtosnowball[[i]])^2;
  var14 = Append[var14, vartemp14];
  , {i, 1, Length[EWSto4]}];
var15 = {};
Do[
  vartemp15 = (1 / Length[EWSto5]) * (EWSto5[[i]] - Warmtosnowball[[i]])^2;
  var15 = Append[var15, vartemp15];
  , {i, 1, Length[EWSto5]}];
var16 = {};
Do[
  vartemp16 = (1 / Length[EWSto6]) * (EWSto6[[i]] - Warmtosnowball[[i]])^2;
  var16 = Append[var16, vartemp16];
  , {i, 1, Length[EWSto6]}];
var17 = {};
Do[
  vartemp17 = (1 / Length[EWSto7]) * (EWSto7[[i]] - Warmtosnowball[[i]])^2;
  var17 = Append[var17, vartemp17];
  , {i, 1, Length[EWSto7]}];
var18 = {};
Do[
  vartemp18 = (1 / Length[EWSto8]) * (EWSto8[[i]] - Warmtosnowball[[i]])^2;
  var18 = Append[var18, vartemp18];
  , {i, 1, Length[EWSto8]}];
var19 = {};
Do[
  vartemp19 = (1 / Length[EWSto9]) * (EWSto9[[i]] - Warmtosnowball[[i]])^2;
  var19 = Append[var19, vartemp19];
  , {i, 1, Length[EWSto9]}];
var110 = {};
Do[
  vartemp110 = (1 / Length[EWSto10]) * (EWSto10[[i]] - Warmtosnowball[[i]])^2;
  var110 = Append[var110, vartemp110];
  , {i, 1, Length[EWSto10]}];
```

In[•]:=
```
var1plot = {};
```

In[•]:=
```
Do[
  plot1temp = (var11[[Length[var11] - i]] + var12[[Length[var12] - i]] +
       var13[[Length[var13] - i]] + var14[[Length[var14] - i]] +
       var15[[Length[var15] - i]] + var16[[Length[var16] - i]] +
       var17[[Length[var17] - i]] + var18[[Length[var18] - i]] +
       var19[[Length[var19] - i]] + var110[[Length[var110] - i]]) / 10;
  var1plot = Prepend[var1plot, plot1temp];
  , {i, 0, 65 - 1}];
```

```
model1 = LinearModelFit[var1plot, x, x]
```

```
pl1 = Plot[model1[x], {x, 0, 62}, PlotStyle → Red];
```

```
plvar1 = ListPlot[var1plot];
```

The autocorrelation of the noisy run with linear regressions:

```
acf[rekke_, τ_] :=
 Mean[Drop[rekke - Mean[rekke], τ] * Drop[rekke - Mean[rekke], -τ]] / Variance[rekke]
```

```
gg11 = Fit[Transpose[{EWSto1, Range[Length[EWSto1]]}][[1 ;; Length[EWSto1]]],
   {zz^2, zz, 1}, zz];
gg12 = Fit[Transpose[{EWSto2, Range[Length[EWSto2]]}][[1 ;; Length[EWSto2]]],
   {zz^2, zz, 1}, zz];
gg13 = Fit[Transpose[{EWSto3, Range[Length[EWSto3]]}][[1 ;; Length[EWSto3]]],
   {zz^2, zz, 1}, zz];
gg14 = Fit[Transpose[{EWSto4, Range[Length[EWSto4]]}][[1 ;; Length[EWSto4]]],
   {zz^2, zz, 1}, zz];
gg15 = Fit[Transpose[{EWSto5, Range[Length[EWSto5]]}][[1 ;; Length[EWSto5]]],
   {zz^2, zz, 1}, zz];
gg16 = Fit[Transpose[{EWSto6, Range[Length[EWSto6]]}][[1 ;; Length[EWSto6]]],
   {zz^2, zz, 1}, zz];
gg17 = Fit[Transpose[{EWSto7, Range[Length[EWSto7]]}][[1 ;; Length[EWSto7]]],
   {zz^2, zz, 1}, zz];
gg18 = Fit[Transpose[{EWSto8, Range[Length[EWSto8]]}][[1 ;; Length[EWSto8]]],
   {zz^2, zz, 1}, zz];
gg19 = Fit[Transpose[{EWSto9, Range[Length[EWSto9]]}][[1 ;; Length[EWSto9]]],
   {zz^2, zz, 1}, zz];
gg110 = Fit[Transpose[{EWSto10, Range[Length[EWSto10]]}][[
    1 ;; Length[EWSto10]]], {zz^2, zz, 1}, zz];
```

```
glatt11 = Table[Max[Flatten[Solve[gg11 == i, zz]][[All, 2]]], {i, 1, 61}];
glatt12 =
  Table[Max[Flatten[Solve[gg12 == i, zz]][[All, 2]]], {i, 1, Length[EWSto2]}];
glatt13 = Table[Max[Flatten[Solve[gg13 == i, zz]][[All, 2]]],
   {i, 1, Length[EWSto3]}];
glatt14 = Table[Max[Flatten[Solve[gg14 == i, zz]][[All, 2]]],
   {i, 1, Length[EWSto4]}];
glatt15 = Table[Max[Flatten[Solve[gg15 == i, zz]][[All, 2]]],
   {i, 1, Length[EWSto5]}];
glatt16 = Table[Max[Flatten[Solve[gg16 == i, zz]][[All, 2]]],
   {i, 1, Length[EWSto6]}];
glatt17 = Table[Max[Flatten[Solve[gg17 == i, zz]][[All, 2]]],
   {i, 1, Length[EWSto7]}];
glatt18 = Table[Max[Flatten[Solve[gg18 == i, zz]][[All, 2]]],
   {i, 1, Length[EWSto8]}];
glatt19 = Table[Max[Flatten[Solve[gg19 == i, zz]][[All, 2]]],
   {i, 1, Length[EWSto9]}];
glatt110 = Table[Max[Flatten[Solve[gg110 == i, zz]][[All, 2]]],
   {i, 1, Length[EWSto10]}];
```

```
y11 = EWSto1[[1 ;; Length[glatt11]]] - glatt11;
y12 = EWSto2[[1 ;; Length[glatt12]]] - glatt12;
y13 = EWSto3[[1 ;; Length[glatt13]]] - glatt13;
y14 = EWSto4[[1 ;; Length[glatt14]]] - glatt14;
y15 = EWSto5[[1 ;; Length[glatt15]]] - glatt15;
y16 = EWSto6[[1 ;; Length[glatt16]]] - glatt16;
y17 = EWSto7[[1 ;; Length[glatt17]]] - glatt17;
y18 = EWSto8[[1 ;; Length[glatt18]]] - glatt18;
y19 = EWSto9[[1 ;; Length[glatt19]]] - glatt19;
y110 = EWSto10[[1 ;; Length[glatt110]]] - glatt110;
```

```
In[•]:= Δt = 11;
cor11 = Table[{t, acf[y11[[t - Δt/2 ;; t + Δt/2]], 1]},
   {t, Δt/2 + 1, Length[y11] - Δt/2}];
cor12 = Table[{t, acf[y12[[t - Δt/2 ;; t + Δt/2]], 1]},
   {t, Δt/2 + 1, Length[y12] - Δt/2}];
cor13 = Table[{t, acf[y13[[t - Δt/2 ;; t + Δt/2]], 1]},
   {t, Δt/2 + 1, Length[y13] - Δt/2}];
cor14 = Table[{t, acf[y14[[t - Δt/2 ;; t + Δt/2]], 1]},
   {t, Δt/2 + 1, Length[y14] - Δt/2}];
cor15 = Table[{t, acf[y15[[t - Δt/2 ;; t + Δt/2]], 1]},
   {t, Δt/2 + 1, Length[y15] - Δt/2}];
cor16 = Table[{t, acf[y16[[t - Δt/2 ;; t + Δt/2]], 1]},
   {t, Δt/2 + 1, Length[y16] - Δt/2}];
cor17 = Table[{t, acf[y17[[t - Δt/2 ;; t + Δt/2]], 1]},
   {t, Δt/2 + 1, Length[y17] - Δt/2}];
cor18 = Table[{t, acf[y18[[t - Δt/2 ;; t + Δt/2]], 1]},
   {t, Δt/2 + 1, Length[y18] - Δt/2}];
cor19 = Table[{t, acf[y19[[t - Δt/2 ;; t + Δt/2]], 1]},
   {t, Δt/2 + 1, Length[y19] - Δt/2}];
cor110 = Table[{t, acf[y110[[t - Δt/2 ;; t + Δt/2]], 1]},
   {t, Δt/2 + 1, Length[y110] - Δt/2}];

In[•]:=
acf1 = {};
Do[
  acf1temp = (cor11[[Length[cor11] - i, 2]] + cor12[[Length[cor12] - i, 2]] +
      cor13[[Length[cor13] - i, 2]] + cor14[[Length[cor14] - i, 2]] +
      cor15[[Length[cor15] - i, 2]] + cor16[[Length[cor16] - i, 2]] +
      cor17[[Length[cor17] - i, 2]] + cor18[[Length[cor18] - i, 2]] +
      cor19[[Length[cor19] - i, 2]] + cor110[[Length[cor110] - i, 2]]) / 10;
  acf1 = Prepend[acf1, acf1temp];
  , {i, 0, 49}];

In[•]:= PL1 = ListPlot[acf1, PlotRange → All, Joined → True];
model1 = LinearModelFit[acf1, x, x]
(model1[60] - model1[0]) / model1[0]
PL2 = Plot[model1[x], {x, 0, Length[acf1]}, PlotStyle → Red];
Show[PL1, PL2]
```

Spatial sensitivity

After finding a stable solution (in this case it it called startclose) use the following cell to perturb it

```
In[•]:= Timing[
 i = 10;
 j = 20;
 L = {};
 Monitor[
  Do[
    center = {i, j};
    Δ1 = 4;
    Δ2 = 8;
    u = 45;
    pertsize = u * A3[[i]];
    pert = Table[0, Length[startclose]];
    pert = Partition[pert, Dimensions[data][[2]]];
    pert[[center[[1]] - Δ1 / 2 ;; center[[1]] + Δ1 / 2, center[[2]] - Δ2 / 2 ;;
       center[[2]] + Δ2 / 2]] = pert[[center[[1]] - Δ1 / 2 ;; center[[1]] + Δ1 / 2,
       center[[2]] - Δ2 / 2 ;; center[[2]] + Δ2 / 2]] + pertsize;
    pert = Flatten[pert];
    startp = Table[
      ToExpression[StringJoin[{ToString[startclose[[k]][[1]]], "==", ToString[
          startclose[[k]][[2]] + pert[[k]]]}]], {k, 1, Length[startclose]}];
    sol = NDSolve[Join[eqliste, startp], Tliste, {t, 0, 5}];
    mean = Mean[(Evaluate[Tliste /. sol] /. t → 5)[[1]]];
    L = Append[L, {i, j, mean}];
    , {i, Δ1 + 1, imax - Δ1, Δ1}, {j, Δ2 + 1, jmax - Δ2, Δ2}];
  , {i, j}];
 Export["Desktop/Lc45.txt", L];]
```

Bibliography

[1] North, G. R. *Analytic solutions to a simple climate model with diffusive heat transport.* J. Atmos, (1975a).

[2] Scheffer, M. (2009) *Critical Transitions in Nature and Society* United Kingdom: Princeton University Press,

[3] North, G. R., Cahalan, R. T. and Coakley, J. A., JR. *Energy balance climate models* Reviews of Geophysics, 19(1):19–121, (1981).

[4] Budyko, M. *The future climte* Eos, Trans. Amer. Geophys. Union, 53, 868-874, (1972)

[5] Held, I. M. and Suarez, M. J. *Simple albedo feedback models of the ice caps* Tellus, 26A, 613-629, (1974).

[6] Budyko, M. *The effects of solar radiation variations on the climate of the Earth*. Tellus, 21(5):611-619, (1969).

[7] Sellers, W. D. *A global climatic model based on the energy balance of the earth- atmosphere system*. Journal of Applied Meteorlogy, 8(3):392-400, 1969.

[8] North, G. R. and Kim, K.-Y.(2017). *Theory of energy-balance climate models* Germany: Wiley-VCH Verlag GmbH Co.

[9] *How did the snowball earths end?* `http://www.snowballearth.org/end.html`

[10] Goddéris, Y.,Hir, G. L., and Donnadieu, Y. *Moddeling the snowball Earth: form its inception to its aftermath* Geological Society, London, Memoirs, v36; p151-161, (2011) doi: 10.1144/M36.10

[11] Paulsen, C. J., Pierrehumbert, R. T., and Jacob, R. L. *Impact of ocean dynamics on the simulation of the neoproterozoic "snowball earth"*. Geophysical Research Letters, 28(8):1575-1578, (2001)

[12] Hoffman, P. F., Kaufman, A. J., Halverson, G. P., and Schrag, D. P. *A neoproterozoic snowball earth.* Science, 281(5381):1342-1346, (1998).

[13] Graves, C. E, Lee,W.-H. and North G. R. *New parameterizations and sensitivities for simple climate models* J. Geophys. Res. 98, 5025-5036, (1993).

[14] North, G. R. *Theory of energy-balance climate models.* Journal of the Atmospheric Sciences,32(11):2033–2043, (1975b)

[15] Wagner, T. J. and Eisenman, I. *False alarms: How early warning signals falsely predict abrupt sea ice loss* Geophysical Research Letters, 42(23):10333-10341, (2015a)

[16] Caesar, L., Rahmstorf, S., Robinson, A., FUeulner, G. and Saba, V. *Observed fingerprint of a weakening Atlantic Ocean overturning circulation* Nature 556, 191-196, (2018)

[17] Ashwin, P., Wieczorek, S., Vitolo, R. and Cox, P. *Tippong point in open systems: bifurcation, noice-induced and rate-dependent examples in the climate* Phil. Trans. R. Soc. A, 370,1166-1184, (2012).

[18] Lenton, T. M., Held, H., Kriegler, E., Hall, J. W., Lutch, W., Ramstor, S. and Schellnuber, H. J. *Tipping elements in the Earth's climate system* PNAS 105 (6) 1786-1793, (2008)

[19] RQ Lin and North, G. R. *A study of abrupt climate change in a simple nonlinear climate model* Climate Dyn. 4: 253, (1990)

[20] Rose, B. E. J and Marshall, J. *Ocean heat transport, sea ice, and multiple climate states: Insights from energy balance models.* Journal of the Atmospheric Scienses, 66(9):2828-2843, (2009)

[21] Leemput, I. A. van de., Wichers, M., Cramer, A. O. J., Borsboom, D., Tuerlinckx, F., ... Scheffer, M. *Critical slowing down as early warning for the onset and termination of depression* PNAS, 111(1), 87-92, (2014)

[22] Ditlevsen, P. D. and Johnse, S. J. *Tipping points: Early warning and wishful thinking* Geophysical Research Letters, VOL. 37, L19703, doi:10.1029/2010GL044486, (2010)

[23] Scheffer, S., Bascompte, J., Brock, W. A., Brovkin, V., Carpenter, S. R., Vasilis Dakos, ... Sugihara, G. *Early-warning signals for critical transitions* Nature 461, 53-59, (2009)

[24] Nes, E. van. and Scheffer, M. *Slow recovery from perturbation as a generic indicator of a nearly catastrophic shift* Am. Nat 169, 738-747, (2007)

[25] Wang, R., Dearing, J. A., Langdon, P. G., Zhang, E., Yang, X.,Dakos V. and Scheffer, M. *Flickering gives early warning signals of a criticaltransition to a eutrophic lake state* Nature, 492, 419–422(2012).

[26] Boettinger. C. and Hastings. A. *Noearly warning signals for stochastic transitions Insights from large deviation theory* Proc. R. Soc. B, 280(1766), 20131372, (2013)

[27] Kefi, S., Dakos, V., Scheffer, M., Nes, E. H. van. and Rietkerk, M. *Early warning signals also precede non-catastrophic transitions* Oikos, 122(5), 641-648, (2013).

[28] Bathiany, S., Bolt, B. van der., Williamson, M. S., Lenton, L. M., Schefer, M., Nes, E. H. van. and Notz, D. *Statistical indicators of Arctic sea-ice stability - prospects and limitations* The Cryosphere, 10, 1631-1645, (2016)

[29] Lenton, T. M. *Early warning of climate tipping points.* Nature Clim. Change, 1(4):201-209, (2011)